2014

FUNCTIONAL ANALYSIS OF THE CELLULOSE SYNTHASE CLASS SPECIFIC REGION IN *PHYSCOMITRELLA PATENS*

Tess Scavuzzo-Duggan
University of Rhode Island, trsduggan@gmail.com

FUNCTIONAL ANALYSIS OF THE CELLULOSE SYNTHASE CLASS SPECIFIC REGION IN *PHYSCOMITRELLA PATENS*

BY

TESS SCAVUZZO-DUGGAN

A THESIS SUBMITTED IN PARTIAL FULFILLMENT OF THE REQUIREMENTS

FOR THE DEGREE OF

MASTER OF SCIENCE

IN

BIOLOGICAL AND ENVIRONMENTAL SCIENCES

UNIVERSITY OF RHODE ISLAND

2014

MASTER OF SCIENCE THESIS

OF

TESS SCAVUZZO-DUGGAN

APPROVED:

Thesis Committee:

Major Professor Alison Roberts

Joanna Norris

Gongqin Sun

Nasser H. Zawia
DEAN OF THE GRADUATE SCHOOL

UNIVERSITY OF RHODE ISLAND
2014

ABSTRACT

Cellulose synthases are found in a wide range of organisms, from bacteria to land plants. However, the cellulose synthases found in land plants (CESAs) form large, multimeric, rosette-shaped cellulose synthase complexes (CSCs) and have three unique regions not found in other cellulose synthases; the N-terminal zinc-binding domain, the Plant Conserved Region (P-CR) and the Class Specific Region (CSR). The CSR, a portion of the large cytoplasmic region that contains the catalytic domain, has been predicted to be involved in CSC formation through *in silico* modeling. This project tested the hypothesis that the CSR is necessary for clade-specific CESA function. We have developed a complementation assay in the moss *Physcomitrella patens* based on the *ppcesa5*KO-2B line, which does not produce gametophores. In *P. patens*, CESAs in the A Clade (CESA3, 5 and 8) have similar CSR structures that are distinct from those in the B Clade (CESA4, 6, 7, 10). The *ppcesa5*KO-2B line is complemented by overexpression of PpCESA3 and PpCESA8, but not by the overexpression of CESAs in Clade B. An overexpression vector containing a Clade A *CESA* with a Clade B CSR was unable to rescue *ppcesa5*KO phenotype, indicating that the CSR is necessary for clade-specific CESA function. However, an overexpression vector containing a Clade B *CESA* with a Clade A CSR was also unable to rescue the *ppcesa5*KO phenotype. This signifies that the CSR is not the sole determinant of clade-specific CESA function. A vector containing a Clade A *CESA* and the C-terminus of a Clade B *CESA* was able to rescue the *ppcesa5*KO phenotype. This suggests that the functionality of the C-terminal region, containing six transmembrane helices, is not a determinant of clade-specific function. A vector containing a Clade A *CESA* with the N-terminus of a Clade B *CESA* was unable to rescue

the *ppcesa5*KO phenotype. This suggests that CSR may be interacting with an N-terminal domain, possibly the P-CR or zinc-binding domain to confer clade-specific function.

ACKNOWLEDGEMENTS

I would like to thank Dr. Alison Roberts for her encouragement and guidance during my tenure not only as a graduate student in her lab, but also as an undergraduate student researcher. Her incredible patience and support have made this degree possible and have greatly impacted my career beyond the University of Rhode Island, for which I am unendingly grateful. I would also like to thank my committee members, Dr. Joanna Norris and Dr. Gongqin Sun for their support as advisors and instructors. Their wisdom both inside and outside the classroom have impacted my education and career on a scale that I never could have imagined. I would like to thank Dr. Candace Oviatt for serving as the Chair for my defense.

I would like to thank Mai Tran for support and guidance with laboratory protocols and for her friendship through a periodically tumultuous degree. I would like to thank XingXing Li for his guidance in optimizing Western blot protocols.

I would like to thank my family and friends for their amazing and seemingly endless belief in my abilities. I would also like to thank them for their understanding during stressful periods in my degree.

This research was supported by The Center for LignoCellulose Structure and Formation, an Energy Frontier Research Center funded by the US Department of Energy, Office of Science, Basic Energy Sciences under award # DE-SC0001090.

This research is based in part upon work conducted using the Rhode Island Genomics and Sequencing Center which is supported in part by the National Science Foundation (MRI Grant No. DBI-0215393 and EPSCoR Grant Nos. 0554548 & EPS-

1004057), the US Department of Agriculture (Grant Nos. 2002-34438-12688 and 2003-34438-13111), and the University of Rhode Island.

TABLE OF CONTENTS

LIST OF FIGURES

LIST OF TABLES

INTRODUCTION

Cellulose Applications

Cellulose is the most abundant biopolymer on earth and is important in a range of applications such as textiles, food and biofuels. Lignocellulosic biofuels are produced in a variety of ways, from thermal conversion to microbial conversion and chemical conversion (Carroll and Somerville 2009). The most cost efficient methods are microbial and chemical conversion. These methods require size reduction of biomass on the submillimeter level, pretreatment to increase accessibility of cell wall polysaccharides, hydrolysis of polysaccharides to simple sugars and conversion of those sugars into fuel, usually ethanol (Carroll and Somerville 2009). One of the main obstacles in efficient cellulosic biofuel production is the recalcitrance of cellulose. As cellulose exists as long microfibrils, cellulases may be prevented sterically from cleaving glycosidic linkages. The cellulose microfibril may additionally prevent hydrolysis due to extensive hydrogen bonding of the glucan chains to one another (Carroll and Somerville 2009). The mechanism of cellulose biosynthesis is still not completely understood, making improvement on cellulose recalcitrance difficult. Thus, it is necessary to understand cellulose structure and synthesis in order to engineer crops better suited for biofuels.

Cellulose Structure

Cellulose occurs as microfibrils composed of hydrogen-bonded β (1, 4)-glucan chains. Cellulose has been characterized as having six different allomorphs, with the first two, cellulose Iα and Iβ, being the native celluloses and the other four, II, III, V, and VI, being chemically and physically altered derivatives (Sturcova et al. 2004; Thomas et al. 2013; Wada et al. 2004). In algae, the Iα and Iβ allomorphs are found with a high degree

of crystallinity, in part due to the large, ribbon-like microfibrillar bundles. In higher plants, these allomorphs predominate, but are more disordered than their algal counterparts, forming thin, ropelike microfibrillar bundles (Sturcova et al. 2004; Thomas et al. 2013; Wada et al. 2004). The exact number of chains in a land plant cellulose microfibril is unknown. Early studies using NMR estimated thirty-six glucan chains in a microfibril (Delmer 1999; Ha et al. 1998; Herth 1983). However, land plant cellulose microfibrils are long, but very thin, making accurate measurements from NMR very difficult. More recent studies, using a combination of NMR with WAXS, SAXS and SANS for more accurate measurement of microfibril diameter, estimate 18-24 glucan chains (Newman et al. 2013; Thomas et al. 2013).

Cellulose Synthases

Cellulose synthases are members of the family 2 glycosyltransferases (GT), characterized by the D, D, D, QXXRW motif (Delmer 1999; Saxena et al. 1995). Cellulose synthases are present in many organisms, from bacteria to land plants. In contrast to bacterial cellulose synthases (BCSs), land plant cellulose synthases (CESAs) have additional domains, including the N-terminal zinc-binding domain, the plant-conserved region (P-CR) and the class-specific region (CSR) (Figure 1) (Arioli 1998; Ihara et al. 1997; Pear et al. 1996). The CSR is notable in that among CESAs of the same class, there is sequence similarity, but between CESAs of different classes, there is little similarity, thus the former designation of hypervariable region (Vergara and Carpita 2001). A recent crystal structure of the bacterial cellulose synthase RsBcsA of *Rhodobacter sphaeroides* confirmed that the conserved D, D, D, QXXRW motif is

responsible for catalysis of β (1, 4)-glucan synthesis using UDP-glucose as a substrate (Morgan et al. 2013).

Cellulose Synthase Complexes

In contrast to BCSs, the CESA subunits aggregate into six-particle rosette-shaped cellulose synthase complexes (CSCs) visible in freeze-fracture electron microscopy of plasma membranes of land plants (Doblin et al. 2002; Kimura et al. 1999; Mueller and Brown 1980) and their closest green algal relatives (Herth 1983). Vascular plants have multiple isoforms of CESAs, with the model plant *Arabidopsis thaliana* containing ten different isoforms (Doblin et al. 2002); three isoforms form CSCs that produce primary cell walls (Desprez et al. 2007; Persson et al. 2007), and three different isoforms form CSCs that produce secondary cell walls (Taylor et al. 2003). Although it is known which CESA isoforms compose the CSCs responsible for either primary or secondary cell wall synthesis in *Arabidposis*, the CESA stoichiometry of rosette CSCs is unknown. The exact number of CESAs in a CSC is also unknown, but it is generally assumed that the number of CESAs in a rosette is equal to the number of glucan chains in a cellulose microfibril. Although previously speculated to contain about thirty six CESAs (Doblin et al. 2002), recent spectroscopic and diffraction data on cellulose microfibrils from celery collenchyma and spruce fibers suggests that CSCs are more likely to contain 18-24 CESAs (Thomas et al. 2013). Sequence analysis has shown that major differences between the six CESA classes, three from primary and three from secondary cell wall CSCs, occur in the CSR (Vergara and Carpita 2001). Taken together with the observation that the CSR is found in CESAs, but not BCSs, this suggests that the CSR plays a role in rosette CSC formation.

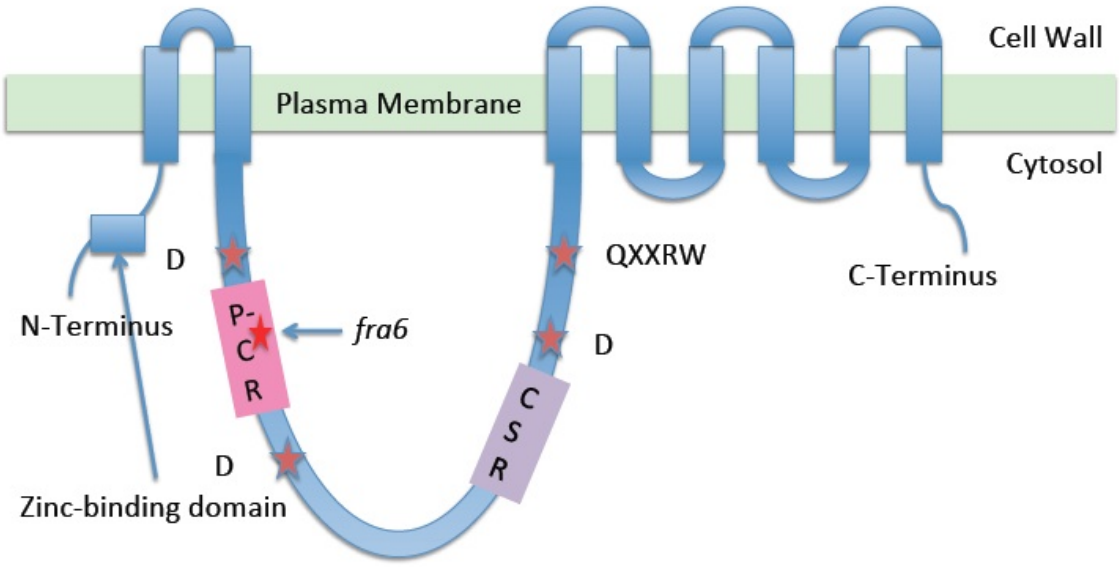

Figure 1: A schematic of an *Arabidopsis thaliana* CESA protein in the plasma membrane. The three unique regions found only in land plant CESAs are marked; the Zinc-binding domain, the P-CR and the CSR. The large cytosolic loop contains the catalytic motif D, D, D, QxxRW, shown with red stars. Also marked is the known mutation in the P-CR of an *AtCESA* known as *fra6*. No mutations have been found in the CSR or zinc-binding domain.

Physcomitrella patens *Cellulose Synthases and the Class-Specific Region*

In the moss *Physcomitrella patens*, there are seven CESA isoforms, which is particularly interesting given that it lacks vascular tissue with secondary cell walls (Roberts and Bushoven 2007). *P. patens* has become established as a model system due to its ease of genetic manipulation. *P. patens* has a fully sequenced genome (Rensing et al. 2008) and has a high rate of homologous recombination, which enables targeted gene modification (Cove 2005). Additionally, a stream-lined process for genetic transformation has been developed and optimized (Roberts et al. 2011). *P. patens* also exists predominantly in the haploid phase of its life cycle, enabling rapid, efficient and facile genetic manipulation (Cove 2005).

Unlike in Arabidopsis, the specific functions of the CESA isoforms in *P. patens* are unknown (Roberts and Bushoven 2007). Whereas Arabidopsis CESAs are specific to primary and secondary cell wall synthesis (Desprez et al. 2007; Persson et al. 2007; Taylor et al. 2003), PpCESAs appear to function in the development of particular tissues (Goss et al. 2012). Additionally, seed plant CSCs contain three CESA isoforms (Desprez et al. 2007; Persson et al. 2007; Taylor et al. 2003), whereas CSCs in *P. patens* could be homo- or hetero-oligomeric (Goss et al. 2012). However, there are two phylogenetically distinct groups of CESAs in *P. patens*, referred to as Clade A and Clade B, which differ in the sequences of their CSRs (Appendix 1, 2) (Goss et al. 2012). Computational modeling indicates that CSRs of Clade B CESAs have a long, central α-helix, whereas in CSRs of Clade A CESAs, this α-helix is disrupted (Sethaphong, personal communication). Previous experiments in which a lesion was inserted into the catalytic region of *PpCESA5* and was thus functionally knocked out indicate that PpCESA5, a

member of Clade A, is expressed in the gametophore and has a striking mutant phenotype in which gametophores fail to develop (Goss et al. 2012). Interestingly, when *ppcesa5*KO-2B was complemented with PpCESA3 or PpCESA8, both in Clade A, the wild-type gametophore phenotype was fully rescued. However, when *ppcesa5*KO-2B was complemented with CESAs from Clade B (PpCESA4, 6, 7, 10), the wild-type phenotype was not rescued (A. Roberts, unpublished). As Clade A and Clade B differ in CSRs, this region may be implicated in the functional differences revealed by the complementation assays. More specifically, the central α-helix found in Clade B CESAs and absent in Clade A CESAs may contribute to CSR-specific function of the CESAs.

Further evidence of CSR function in CSC formation is demonstrated by the recent computational modeling of the *Gossypium hirsutum* CESA1 cytosolic domain. The catalytic residues of the GhCESA1 computational model align closely with that of the RsBcsA crystal structure, indicating that the catalytic mechanism is conserved across family 2 GTs and validating the computational model (Sethaphong et al. 2013). This model depicts the P-CR and CSR as facing away from the catalytic region into the cytoplasm, indicating that these regions may be involved in CSC formation. Models created using the program Rosetta Symmetry (Rohl et al. 2004) predict that the P-CR and CSR interact when the CESAs form dimers, trimers and hexamers (Sethaphong et al. 2013). A missense mutation in the P-CR of *Arabidopsis thaliana* leads to a decrease in cellulose deposition and wall thickness in fiber cell walls (Zhong et al. 2003), indicating that the P-CR is necessary for cellulose synthesis (Figure 1). However, no known mutations that affect cellulose biosynthesis are located in the CSR (Sethaphong et al. 2013). Coupled with evidence that Arabidopsis primary and secondary CSC components

differ in CSR structure and that CSR structure is correlated with the ability of *P. patens* CESAs to complement the *ppcesa5* mutant, the computational model of GhCESA1 suggests that the CSR plays a direct role in CSC formation.

In this study, I analyzed the role of the CSR in the functional differences between Clade A and Clade B CESAs in gametophore development using the *ppcesa5*KO-2B complementation system. By complementing *ppcesa5*KO-2B with a chimeric CESA5 containing the CSR from a Clade B CESA (CESA4), I determined that the ability of Clade A CESAs to complement the *ppcesa5*KO phenotype is dependent on the CSR. By complementing *ppcesa5*KO-2B with a chimeric CESA4 containing the CSR of a Clade A CESA (CESA5), I determined that the CSR is not the only region necessary for clade-specific CESA function. By complementing *ppcesa5*KO-2B with a chimeric CESA5 containing the C-terminus of CESA4, I determined that the C-terminus is not necessary for clade-specific function. By complementing *ppcesa5*KO-2B with a chimeric CESA5 containing the N-terminus of CESA4, I determined that the N-terminus, including the zinc-binding domain and P-CR, is necessary for clade-specific function.

MATERIALS AND METHODS

Vector Construction

General Strategy

Chimeric CESA expression vectors were constructed using PCR fusion and Invitrogen MultiSite Gateway cloning (Life Technologies, Grand Island, NY, USA). *PpCESA8, PpCESA4* and *PpCESA5* cDNA clones were used as templates for PCR. PCR products were fused by a single overlap extension to produce chimeric CESAs (Atanassov et al. 2009), which were inserted with a triple hemagglutinin tag into the pTHAct1Gate (xt18) destination vector containing an actin1 promoter driving constitutive expression and sequences that target the expression vector to the *P. patens* 108 locus, which can be disrupted without producing a phenotype (Perroud and Quatrano 2006).

PCR Fusion

PCR fusion was carried out as described by Atanassov (Atanassov et al. 2009) with modifications (Appendix 3). Instead of amplifying into *attL* sites, which recombine into expression vectors, chimeric CESAs were amplified into *attB* sites, which recombine into entry clones. PCR primers were designed containing twelve nucleotides of shared sequence (overlap region) and fifteen nucleotides of upstream or downstream sequence from *PpCESA4*, *PpCESA5* or *PpCESA8* (Figure 2, Table 1). CesaXattB5 and SR1 (F1), SF1 and SR2 (F2), or CesaXattB2 and SF2 (F3) primers were combined into three separate 50 µl PCR reactions with Phusion polymerase (New England Biolabs, Ipswich, MA, USA) and *PpCESA4, 5,* or *8* cDNA clones pdp39044, pdp21409, and pdp24095, respectively (RIKEN BRC, http://www.brc.riken.jp/lab/epd/Eng/), as previously

Table 1. Primers used to amplify fragments for constructing chimeric CESAs.

Primer Name	Primer Sequence
CesA5attB5	GGGGACAACTTTGTATACAAAAGTTGCGATGGAGGCTAATGCAGGCCTTAT
CesaA5attB2	GGGGACCACTTTGTACAAGAAAGCTGGGTACTAACAGCTAAGCCCGCACTCGAC
CesA4CDSattB5	GGGGACAACTTTGTATACAAAAGTTGTCATGAAGGCGAATGCGGGGCTGTT
CesA4CDSattB2	GGGGACCACTTTGTACAAGAAAGCTGGGTACTATCGACAGTTGATCCCACACTG
CesA5CSR4 SF1	GTATATGTAGGCACGGGATGCTGTTTCAAGAGGCGA
CesA5CSR4 SF2	AATCCTGGGTCATTGTTGAAGGAGGCAATTCACGTC
CesA5CSR4 SR1	TCGCCTCTTGAAACAGCATCCCGTGCCTACATATAC
CesA5CSR4 SR2	GACGTGAATTGCCTCCTTCAACAATGACCCAGGATT
CesA5CSR8 SF1	GTATATGTAGGCACGGGATGTGTCTTTAGGAGGCAA
CesA5CSR8 SF2	AGCGCGGGCTCCCTCCTCAAGGAGGCAATTCACGTC
CesA5CSR8 SR1	TTGCCTCCTAAAGACACATCCCGTGCCTACATATAC
CesA5CSR8 SR2	GACGTGAATTGCCTCCTTGAGGAGGGAGCCCGCGCT
CesA4CSR5 SF1	GTTTATGTGGGTACGGGGACTGTGTTCAACAGGAAG
CesA4CSR5 SF2	AGCCCGGGATCTCTTCTCAAGGAGGCAATTCATGTG
CesA4CSR5 SR1	CTTCCTGTTGAACACAGTCCCCGTACCCACATAAAC
CesA4CSR5 SR2	CACATGAATTGCCTCCTTGAGAAGAGATCCCGGGCT
CesA5CSR3 SF1	GTATATGTAGGCACGGGATGCGTGTTCAGGAGGCAA
CesA5CSR3 SF2	AGCGCGGGCTCACTCCTCAAGGAGGCAATTCACGTC
CesA5CSR3 SR1	TTGCCTCCTGAACACGCATCCCGTGCCTACATATAC
CesA5CSR3 SR2	GACGTGAATTGCCTCCTTGAGGAGTGAGCCCGCGCT

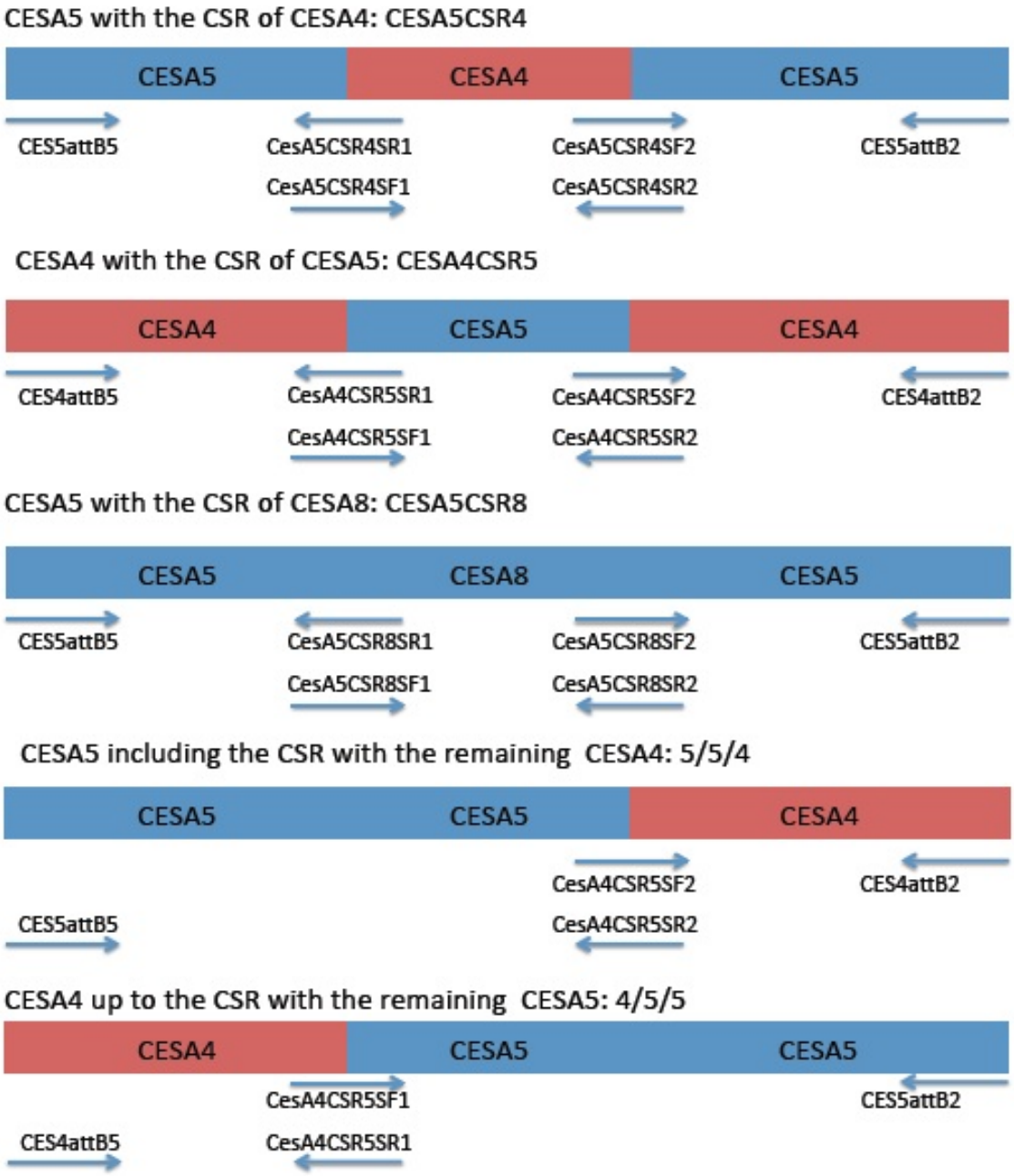

Figure 2. A schematic detailing the primer design for each chimera and nomenclature of the chimeric CESAs.

described (Atanassov et al. 2009). PCR products were run with a calibrated ladder (New England Biolabs) on a 1% agarose gel containing 0.5 µg/ml ethidium bromide at 100 V for 20 minutes and imaged to estimate the concentration. PCR products F1 (400 ng), F2 (80 ng), and F3 (200 ng) were combined in a 30 µl PCR fusion reaction with Phusion polymerase (New England Biolabs) (Figure 3) and no primers. PCR fusion products were purified according to the Invitrogen MultiSite Gateway Pro kit (Life Technologies) and resuspended in 7 µl of 1X TE.

MultiSite Gateway Cloning

Expression vectors were constructed using the MultiSite Gateway Pro kit (Life Technologies). To construct entry clones, fusion products containing *attB* sites were cloned into Invitrogen pDONR P5-P2 (Life Technologies). Plasmid DNA was purified from kanamycin resistant colonies using a QIAGEN QIAPrep Spin Miniprep kit according to manufacturer's instructions (QIAGEN Inc, Valencia, CA, USA). Plasmids were digested with EcoRI-HF and EcoRV-HF restriction enzymes (New England Biolabs) selected to produce a chimera-specific digestion pattern. Clones with the predicted digestion pattern were confirmed by sequencing on the Applied Biosystems 3130xl genetic analyzer using Applied Biosystems BigDye Terminator v3.1 chemistry (Life Technologies) using gene-specific primers (Table 2). Entry clones and an Invitrogen pDONR P1-P5r (Life Technologies) entry clone containing a triple hemagglutinin tag were cloned into the pTHAct1Gate, referred to here as xt18 (Perroud and Quatrano 2006), destination vector. Plasmid DNA was purified from ampicillin resistant colonies as previously described and digested with the SwaI restriction enzyme(New England Biolabs). Plasmids with the predicted digestion pattern were tested

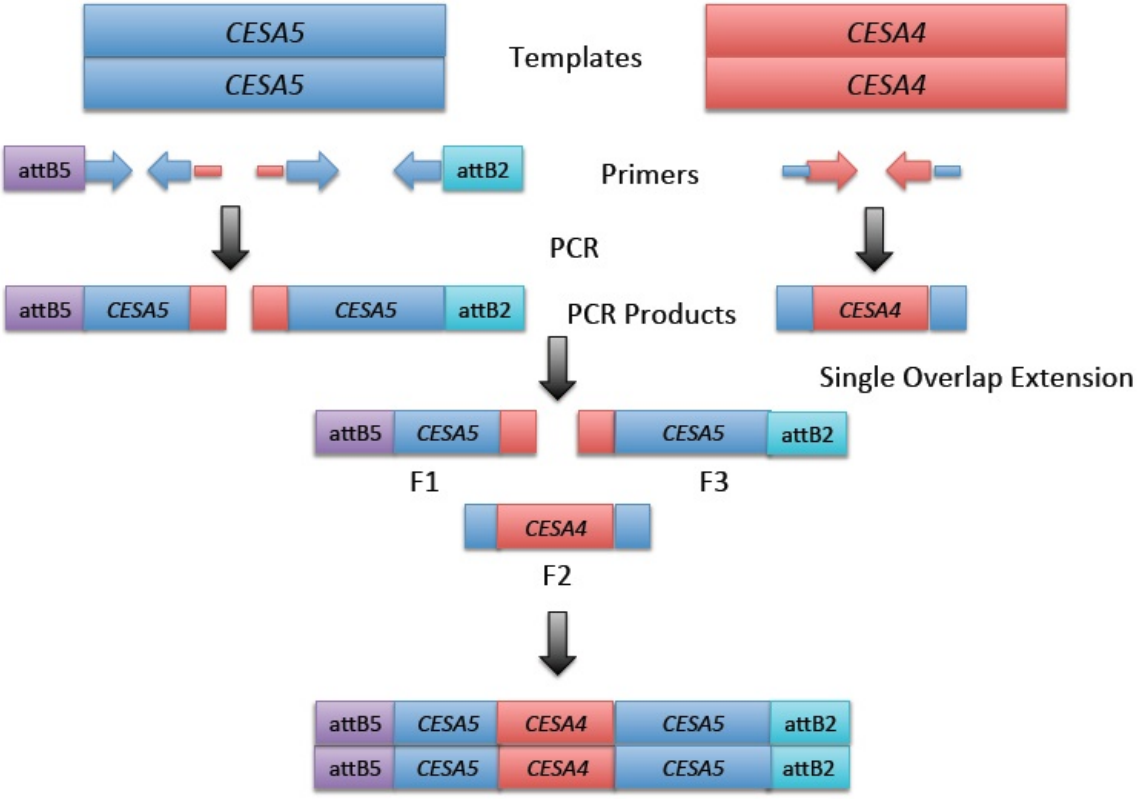

Figure 3. A schematic of PCR fusion adapted from Atanassov et al (Atanassov et al. 2009). Using *PpCESA* cDNA as templates, F1, F2 and F3 fragments were amplified by PCR for the final overlap extension step to create chimeric *Ppcesa* PCR products.

Table 2. Primers used for sequencing CESA chimeras.

Primer Name	Primer Sequence
P99	CCCGTTTTTGAAAGGTCTGA
P101	CAGTGTGGGATCAACTGTCG
P117	CCTTATTGCAGGCTCACACA
P118	CGTACATCAACGCCACAATC
P119	TTCTTACAGATGGCACCGT
P143	TTTGGACGATGACTCTCACG
P146	CCCTTTGTGGTACGGGTATG
P153	GATTTTGGATCAGTTCCCGA
P155	CCATGCTGACCTTTGAGGTT
P373	CCACAACACTGTCTTCTTCGAC
P374	TGATACAGGTCTTTCTGGGACA
P395	GAGCTATGGTGGCAATTACGAC
P403	CTTTCTCTCGATTTTCGTGACC
P404	TGACACGGAAGTGATGCTATCT
P405	AGTAATTTGGCGAGTCTGTGGT

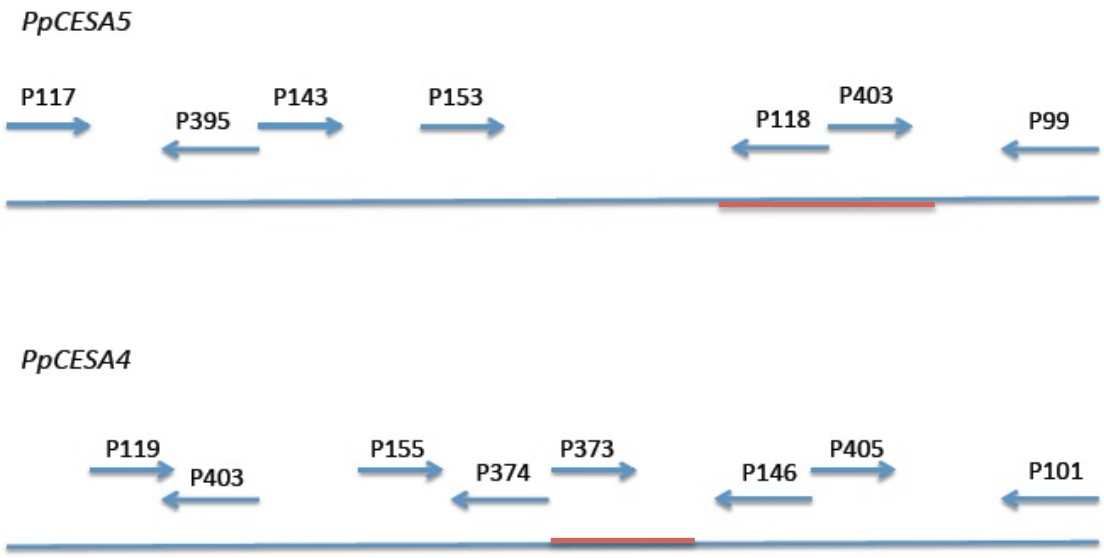

Figure 4. A schematic of sequencing primers in relation to *PpCESA5* and *PpCESA4* gene sequences. CSR shown in red.

for correct recombination by sequencing with primers P395 and P403 for *PpCESA5* constructs and P404 and P405 for *PpCESA4* constructs (Table 2, Figure 4).

Expression Clone Preparation

Plasmid DNA from sequence-verified expression clones was isolated using GenElute HP Plasmid Midiprep kit (Sigma-Aldrich, St. Louis, MO, USA) or NucleoBond Midiprep Xtra kit (Macherey-Nagel Inc., Bethlehem, PA, USA) according to the manufacturer's instruction. 100 µg of plasmid DNA was linearized using 50 activity units of SwaI restriction enzyme (New England Biolabs) in a 110 µl reaction, ethanol precipitated and resuspended in sterile 5 mM Tris-Cl at 1 µg/µl.

Moss Subculture

Protonemal filaments from the *P. patens cesa5*KO-2 line (Goss et al. 2012) provided by Dr. Alison Roberts (University of Rhode Island, Kingston, RI, USA) were grown on BCDAT overlain with cellophane at 25°C with fluorescent lights at a photon flux density of 60 µM $m^{-2}s^{-1}$ for 7 d. The tissue was then homogenized using Omni International hard tissue omni tip probes (USA Scientific, Ocala, FL, USA) in 4-6 ml of sterile water and plated on BCDAT overlain with cellophane and grown under the same conditions for 5-6 d for protoplast isolation according to Roberts et al (2011).

Protoplast Isolation & Transformation

Protoplasts were isolated according to Roberts et al (2011) using the *P. patens cesa5*KO-2 line. Briefly, protonemal tissue was digested using driselase, washed thrice in an isosmotic medium, mixed with the linearized expression vector and polyethylene glycol and heat shocked at 45°C for three minutes. Protoplasts were resuspended in top agar protoplast regeneration medium (PRMT) and plated on bottom agar protoplast

regeneration medium (PRMB) overlain with cellophane. Transformed protoplasts were screened through two rounds of hygromycin selection to obtain stable transformants.

Complementation Assays

Stably transformed moss lines were arrayed on BCDAT plates and incubated at 25°C with fluorescent lights at a photon flux density of 60 μM $m^{-2}s^{-1}$ for 7 d. A dissecting microscope was used at 20X - 40X to count the number of lines producing gametophores and to assess gametophore development and phyllotaxy. The Leica M165 FC dissecting microscope was used to examine lines and individual gametophores between 4.6 and 63X (Leica Microsystems Inc, Buffalo Grove, IL, USA). The Olympus BH2-RFCA compound microscope was used to examine individual leaves at 312.5X (Olympus Corporation, Lake Successs, NY, USA). Images were captured using a Leica BFC310 FX camera (Leica Microsystems Inc, Buffalo Grove, IL, USA). Lines resulting from transformation with chimeric CESA expression vectors were compared to lines resulting from transformation with a positive control vector (*PpCESA5*::*ppcesa5*KO-2) and a negative control vector (the destination vector without the Gateway cassette transformed into *ppcesa5*KO-2).

Statistics

P values were assigned using the Two-Tailed Fisher's Exact Test of Independence (Sokal and Rohlf 1981). For each expression vector, data from each trial was pooled and compared against the corresponding opposite control data (i.e. a vector that did not rescue would be compared against the positive control) to determine the p value. Each expression vector was compared against the corresponding similar control to determine whether or not there was a significant difference.

Protein Isolation

Microsomal proteins were isolated from at least twelve lines from each non-rescuing transformation along with 3XHACESA8 lines (positive control) and xt18-GW lines (negative control) according to Hutton et al (Hutton et al. 1998) with modifications. Tissue was ground using the Argos pellet mixer and pestle (Argos Technologies Inc., Elgin, IL, USA) in 100 µl of extraction buffer containing 50 mM HEPES, 0.5 M sucrose, 0.1 mM EDTA, and 4 mM M-ascorbic acid for five minutes on ice. The lysate was centrifuged at 10,000 x g for ten minutes at 4° C and the supernatant centrifuged again under the same conditions in order to remove plastids and nuclei. The final supernatant was collected and centrifuged at 100,000 x g for thirty minutes at 4°C and the pellet was resuspended in 15 µl 2X SDS buffer and 15 µl of deionized water.

Protein Quantification

Protein extractions were quantified using the Pierce BCA Protein Assay kit (Thermo Scientific Inc., Rockford, IL, USA) according to manufacturer's instructions, using 25 µl of each standard and 7-10 µl of each unknown. Proteins run on the NuPAGE 4-12% Bis-Tris gel (Thermo Scientific Inc.) were normalized according to the protein sample with the lowest concentration from the BCA Protein Assay (Thermo Scientific Inc.).

Western Blot

At least 10 ng of each protein sample was run on a NuPAGE 4-12% Bis-Tris gel (Thermo Fisher Scientific Inc.) at 50 mV for 15 minutes and then 200 mV for 30 minutes. The gel was soaked in 1X transfer buffer (0.2 M glycine, 0.025 M Tris base) for 10 min at 4° C and then transferred onto a polyvinylidene difluoride membrane (Thermo

Scientific Inc.) using the BioRad Mini-PROTEAN II Electrophoresis Cell (Bio-Rad Life Sciences, Hercules, CA, USA) at 75 V for one hour at 4° C. The membrane was blocked by incubating with shaking at 80 rpm in 5% (w/v) milk in 1X TBST (50 mM Tris, 150 mM NaCl, 0.05% Tween 20) for one hour at 25° C and washed with 1X TBST. The membrane was then incubated with shaking at 80 rpm in 5% (w/v) milk in TBST with 1:1000 anti-hemagglutinin antibody (HA11 Clone 16B12, Covance, Dedham, MA, USA) overnight at 4° C and washed four times with 1X TBST for four minutes at 80 rpm. The membrane was then incubated with shaking at 80 rpm in 5% (w/v) milk in 1X TBST with 1:200 anti-mouse IgG peroxidase antibody for one hour at 25° C and washed four times with 1X TBST for 4 minutes at 80 rpm. 2-3 ml of Substrate A & B from the Pierce ECL Western Blotting Substrate kit (Thermo Scientific Inc.) were applied to the membrane and incubated for one minute. Membranes were exposed for 20 minutes using X-ray film (Research Products International, Mount Prospect, IL, USA). Blots were subsequently incubated with shaking at 80 rpm in 5% (w/v) milk in TBST with 1:500 anti-tubulin antibody (Monoclonal Anti-α-TubulinClone DM1A, Sigma-Aldrich, St. Louis, MO, USA) overnight at 4° C. The membrane was washed as previously described and incubated with shaking at 80 rpm in 5% (w/v) milk in 1X TBST with 1:200 anti-mouse IgG peroxidase antibody for one hour at 25° C. Finally, the membrane was washed as previously described, blotted and exposed using X-ray film (Research Products International) after 20 minutes.

RESULTS

Experimental Design

The *ppcesa5*KO-2B complementation assay was developed to test the role of the CSR in clade-specific CESA function in *P. patens*. The *ppcesa5*KO mutants are characterized by an inability to form normal gametophores, most commonly developing abnormal buds and rarely producing small gametophores with irregular phyllotaxy (Goss et al. 2012). *PpCESA*s within the same clade (Clade A) can rescue the *ppcesa5*KO phenotype but *PpCESA*s from Clade B cannot (Roberts, unpublished). By transforming the *ppcesa5*KO-2B line with expression vectors containing various *PpCESA* chimeras and scoring for complementation of the mutant phenotype, I tested the hypothesis that a Clade A CSR is necessary and sufficient for Clade A-specific CESA function in gametophore development. Based on this hypothesis, I predicted that a Clade A CESA with the CSR of a Clade B CESA would be unable to rescue the *ppcesa5*KO phenotype, whereas a Clade A CESA with the CSR of another Clade A CESA would be able to rescue the phenotype. Additionally, I predicted that if the CSR is sufficient for clade-specific function, then a Clade B CESA with the CSR of a Clade A CESA would also be able to rescue the *ppcesa5*KO phenotype. The chimeric *PpCESA*s designed to test these predictions were fused with a triple hemagglutinin tag so that the resulting moss transformants could be tested for expression of the transgene. In the complementation assays, *ppcesa5*KO-2B lines were transformed with three separate expression clones along with a positive control vector containing the wild-type *PpCESA5* and negative empty vector control. Stable transformants were arrayed on solid medium and scored for gametophore development. Results were included if they met several criteria, the first

being a minimum number of five stable lines per expression clone transformation. Results were excluded if the positive and/or negative control was absent or produced too few lines (a result of either a low transformation rate or contamination). Results were also excluded if the positive and/or negative control behaved abnormally (i.e the positive control produced gametophores in less than 40% of stable, transformed lines).

Transformation with Positive and Negative Control Vectors

The *ppcesa5*KO phenotype is characterized by a complete absence of leafy gametophores, or occasionally stunted gametophores with abnormal phyllotaxy. *PpCESA5*KO lines typically produce cellulose deficient buds that are unable to mature into normal leafy gametophores due to irregularities in cell expansion and cell division (Goss et al. 2012). The gametophores that are able to develop from these irregular buds are small, producing only one to three irregularly spaced, misshapen leaves. Transformation with a 3XHA*PpCESA5* expression vector fully and reproducibly rescued the *ppcesa5*KO phenotype. Between 40% and 100% of lines stably transformed with this vector produced gametophores, with an average of 74% of lines producing gametophores, and each line that produced gametophores also produced a full length protein when probed with an anti-hemagglutinin antibody (Table 3, Figures 5, 6 & 7). These lines produced several gametophores (usually more than four per colony) of normal size and phyllotaxy, with leaves occurring in a regular spiral pattern (Figure 8). Leaves were narrow and pointed with elongated cells occurring in distinct files (Figure 8). Transformation with the xt18-GW empty vector consistently failed to rescue the *ppcesa5* KO phenotype. Between 0% and 20% of lines produced gametophores, with an average of 5% of lines producing gametophores (Table 3, Figure 5 & 7). Gametophores produced

by xt18-GW lines resembled those of the *ppcesa5*KO-2B line. Each line that produced gametophores typically only produced one or two per colony. The gametophores themselves were small, with only one to three misshapen, small leaves. The leaves were composed of irregularly shaped cells and lacked the conducting cells present in mature leaves and gametophores (Figure 8).

The Class-Specific Region in Clade-Specific Function

Transformation with a vector containing *CESA5* with the CSR of another Clade A *CESA* (3XHA*ppcesa5CSR8*) was able to rescue the *ppcesa5*KO phenotype, producing normal gametophores in the same numbers as 3XHA*PpCESA5* transformed moss lines ($p < 0.0001$, Figure 5 A, Table 3). The ability of 3XHA*ppcesa5CSR8* to rescue the *ppcesa5*KO phenotype indicates that CSRs within the same clade can perform clade-specific functions in Clade A CESAs.

Transformation with a vector containing *CESA5* with the CSR of a Clade B *CESA* (3XHA*ppcesa5CSR4*) failed to rescue the *ppcesa5*KO phenotype, producing no gametophores in both trials ($p < 0.0001$, Figure 5 B, Table 3). This was consistent with the negative control, xt18-GW transformations, which rarely produced gametophores that tended to be stunted with an abnormal phyllotaxy (Figure 5 A, Table 3, Figure 8), similar to the *ppcesa5*KO phenotype (Goss et al. 2012).

Transformation with a vector containing a Clade B *CESA* with the CSR of a Clade A *CESA* (3XHA*ppcesa4CSR5*) also failed to rescue the *ppcesa5*KO phenotype, producing low numbers of lines with stunted, abnormal gametophores in both trials ($p < 0.0001$, Figure 5 C, Table 3), consistent with the negative control and the *ppcesa5*KO phenotype (Goss et al. 2012).

Table 3. Summary of chimeric *CESA* expression clone-transformed *ppcesa5* KO-2 moss lines producing gametophores. The positive and negative controls of each trial are included. All data are shown with indication of which trials were included in the analysis.

Expression Clone	Trial No.	Lines with Gametophores	Positive Control with Gametophores	Negative Control with Gametophores	Included in Statistical Analysis
Ppcesa5CSR4	1	0/9	11/27	5/65	Yes
Ppcesa5CSR4	2	0/20	11/18	0/20	Yes
Ppcesa5CSR4	3	0/4	1/8	12/25	No
Ppcesa5CSR4	4	0/14	3/12	0/15	No
Ppcesa4CSR5	1	3/33	21/24	2/51	Yes
Ppcesa4CSR5	2	0/11	9/13	0/30	Yes
Ppcesa4CSR5	3	0/6	0	0	No
Ppcesa5CSR8	1	9/14	19/24	2/21	Yes
Ppcesa5CSR8	2	3/4	15/15	0/12	No
Ppcesa5CSR8	3	10/15	6/10	1/5	Yes
Ppcesa5CSR8	4	3/6	4/4	0/4	No
Ppcesa5CSR8	5	0/6	0/4	0/4	No
Ppcesa4/5/5	1	1/21	9/13	0/30	Yes
Ppcesa4/5/5	2	1/14	15/15	0/12	Yes
Ppcesa5/5/4	1	6/15	19/24	2/21	Yes
Ppcesa5/5/4	2	2/6	3/4	2/4	No
Ppcesa5/5/4	3	2/8	15/15	0/12	Yes
Ppcesa5/5/4	4	15/43	23/33	1/21	Yes

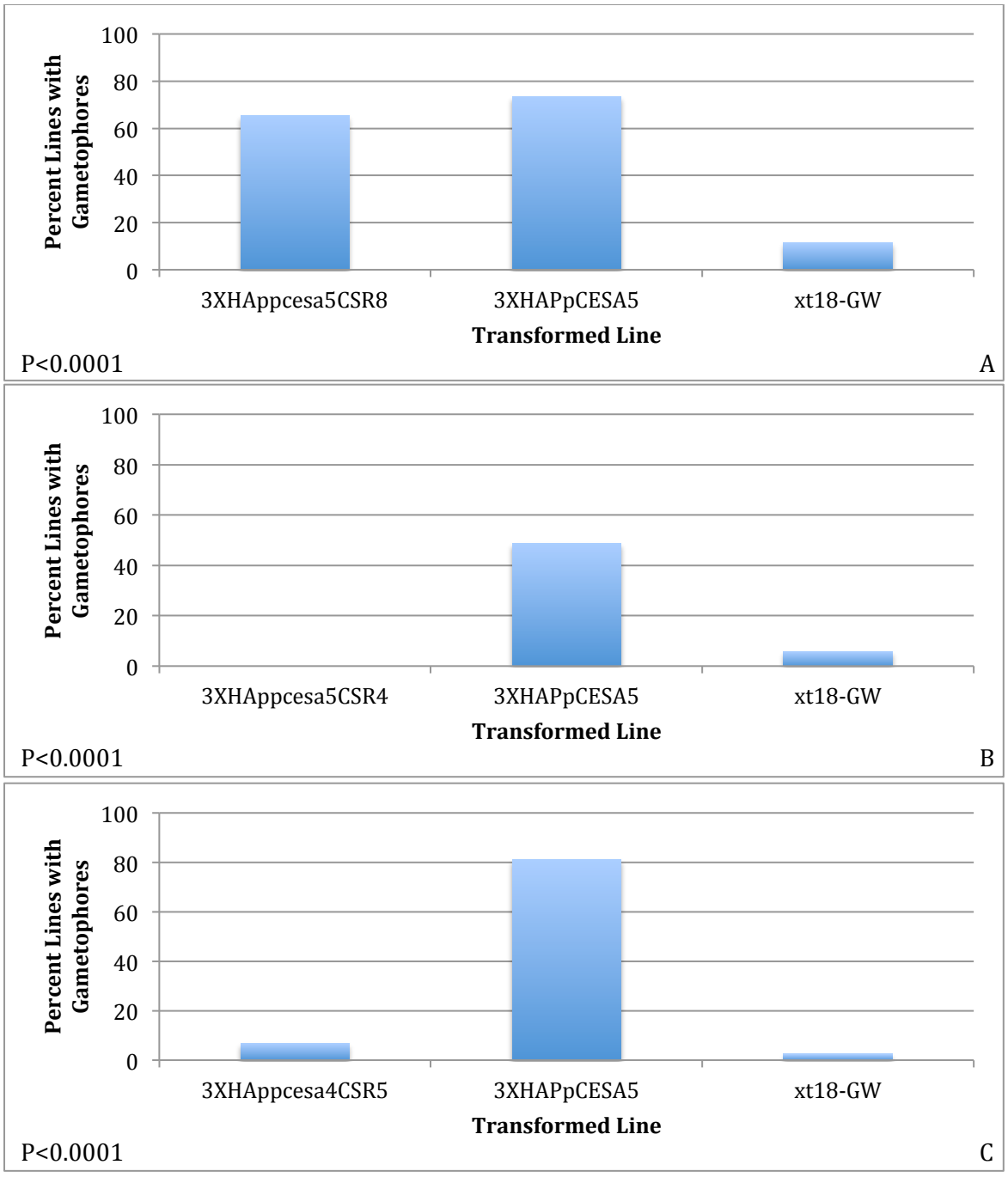

Figure 5. *Ppcesa5*KO-2B phenotypic rescue by *PpCESA* CSR swap vectors and corresponding positive and negative control vectors. Data from replicate trials was pooled for graphical representation and statistical analysis using the two-tailed Fisher exact probability test. (A) Vector containing Clade A CESA with Clade A CSR. (B) Vector containing Clade A CESA with Clade B CSR. (C) Vector containing Clade B CESA with Clade A CSR. Chart detailing individual trials of each CSR swap presented in Appendix 4.

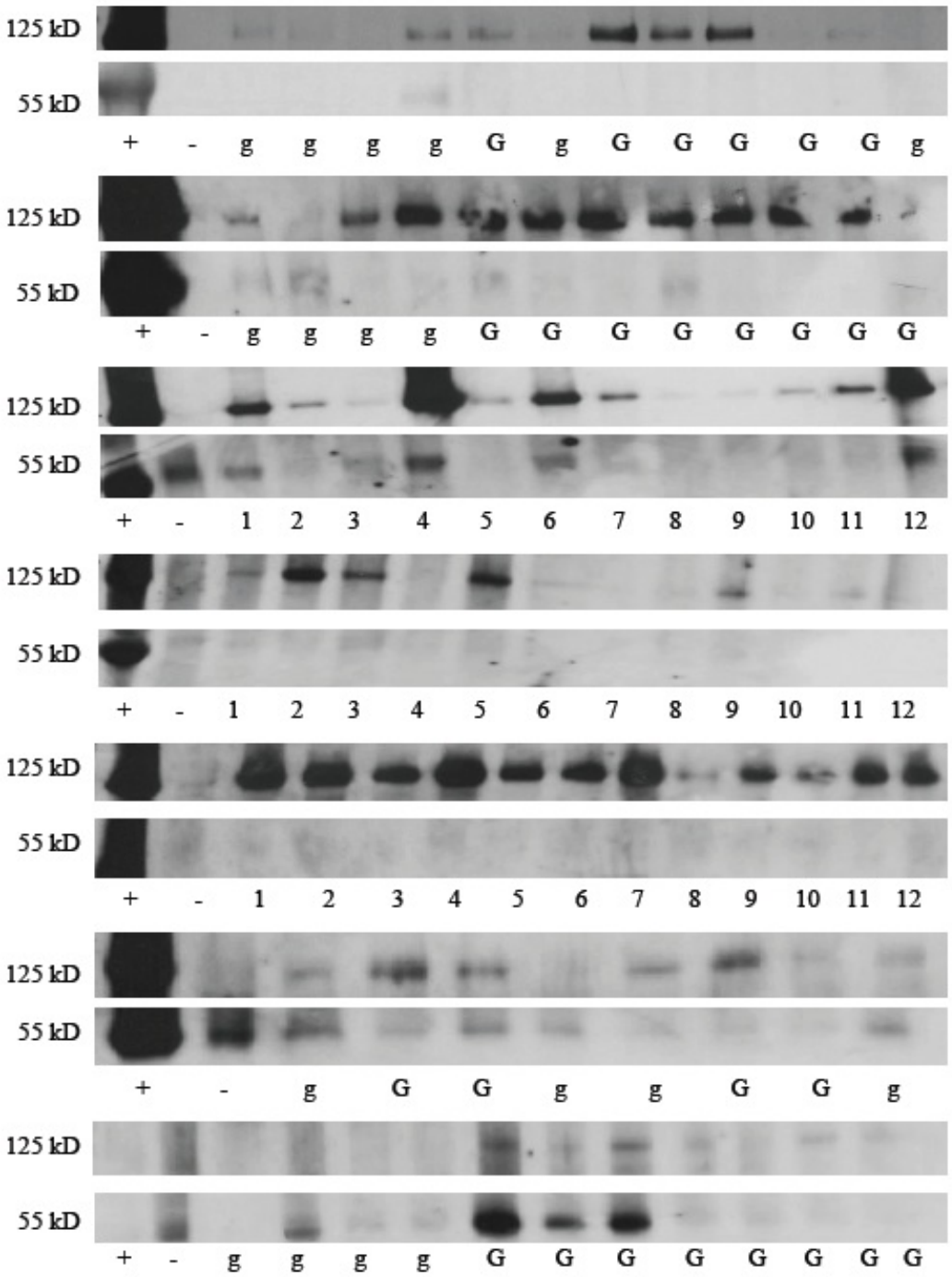

Figure 6. Western blots of microsomal protein extracts from *ppcesa5*KO-2B lines transformed with expression vectors containing various 3XHA-CESA fusions. Blots probed with anti-HA probe are above blots probed with anti-tubulin probe. + = positive control (*3XHAPpCESA8*) - = negative control (xt18-GW). G = lines with normal gametophores; g = lines without gametophores. Numbered lines did not produce gametophores. From top to bottom: 3XHA*PpCESA5*, 3XHA*PpCESA5,* 3XHA*ppcesa4CSR5*, 3XHA*ppcesa5CSR4*, 3XHA*ppcesa4/5/5*, 3XHA*ppcesa5/5/4*, and 3XHA*ppcesa5/5/4*. Uncropped Western blots can be found in Appendix 5.

To test whether failure to rescue the *ppcesa5*KO phenotype could be explained by poor expression or misfolding and subsequent destruction of proteins coded by the transgenes, transformants that did not rescue the *ppcesa5*KO phenotype were analyzed for accumulation of the transgenic protein through Western blots probed with an anti-hemagglutinin antibody and an anti-tubulin antibody to evaluate protein loading. Initially, Western blots were performed on microsomal protein extracts from 3XHA*PpCESA5* transformed moss lines that both produced and did not produce gametophores (Figure 6). All lines that produced gametophores showed the predicted band at 125 kD, indicating that the full-length 3XHA*PpCESA5* protein was expressed. Six lines that did not produce gametophores produced the predicted band and the other four lines did not. One interpretation of this result is that a minimum dose of PpCESA5 proteins is needed to successfully rescue the *ppcesa5* KO phenotype. It is also possible that some of the stable transformants do not contain the intact vector, as evidenced by the lack of a 125 kD band in most of the gametophore-less lines, instead containing an truncated vector with the functional resistance cassette.

Tubulin bands across the Western blots were often faint and of variable intensity, indicating that protein loading was uneven. Despite using the Pierce BCA Protein Assay, protein concentrations were too low to measure accurately. Additionally, a linear trend line was used initially to calculate protein concentration against BSA standards instead of the recommended exponential trend line. Both of these factors contributed to inconsistent protein loading, as indicated by variable tubulin levels across the blots (Figure 6). Using larger quantities of moss tissue to increase protein concentration of the samples will make calculating protein concentration more reliable.

All 3XHA*ppcesa4CSR5* lines produced the predicted band at 125 kD, indicating that the full-length protein was expressed (Figure 6). This expression validates the inability of 3XHA*ppcesa4CSR5* to rescue the *ppcesa5* KO phenotype. In contrast, only seven out of twelve 3XHA*ppcesa5CSR4* transformed lines produced the predicted band at 125 kD (Figure 6). However, this still indicates that full-length 3XHA*ppcesa5CSR4* is unable to rescue the *ppcesa5* KO phenotype. The lower apparent expression rate may be due to uneven protein loading, as in this particular Western blot, a fainter anti-HA band correlated to a fainter anti-tubulin band (Figure 6). Regardless, the Western blots indicated that the chimeric proteins were intact and not truncated, indicating that failure to rescue cannot be solely attributed to lack of protein expression.

The N and C-termini in Clade-Specific Function

In order to determine other regions necessary in clade-specific CESA function in *P. patens*, N and C-terminal swaps were created between *PpCESA5 and PpCESA4.* The C-terminal swap termed 3XHA*ppcesa5/5/4* consisted of the C-terminus of *PpCESA4* after the CSR fused onto the N-terminus of *PpCESA5* up to and including the CSR. The N-terminal swap termed 3XHA*ppcesa4/5/5* consisted of the N-terminus of *PpCESA4* up to the CSR fused onto the C-terminus of *PpCESA5* from the CSR onwards. The *ppcesa5*KO phenotype was not rescued in 3XHA*ppcesa4/5/5* transformed lines, with only one line in each trial producing stunted gametophores with abnormal phyllotaxy, consistent with the *ppcesa5*KO phenotype (Figure 7, Table 3) (Goss et al. 2012). The *ppcesa5*KO phenotype was rescued in some 3XHA*ppcesa5/5/4* transformed lines, but not in the same numbers as the positive control (Figure 7, Table 3), possibly indicating a partial rescue.

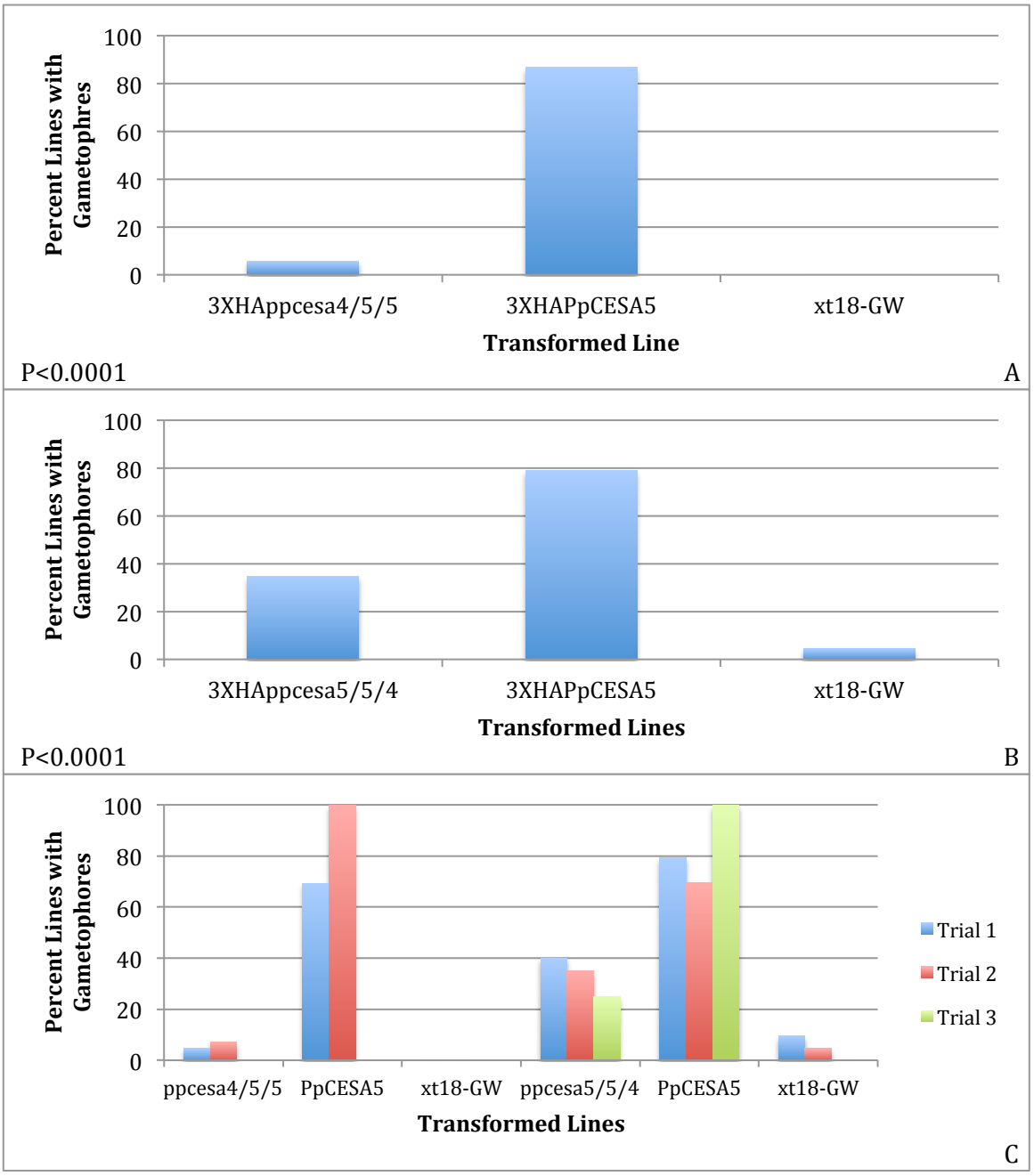

Figure 7. *Ppcesa5*KO-2B phenotypic rescue by each N- and C-terminal swap mutant and corresponding positive and negative control vectors. Data from replicate trials was pooled for graphical representation and statistical analysis using the two-tailed Fisher exact probability test. (A) Vector containing Clade A CESA with N-terminus of Clade B CESA. (B) Vector containing Clade A CESA with C-terminus of Clade B CESA. (C) Individual trials of both vectors.

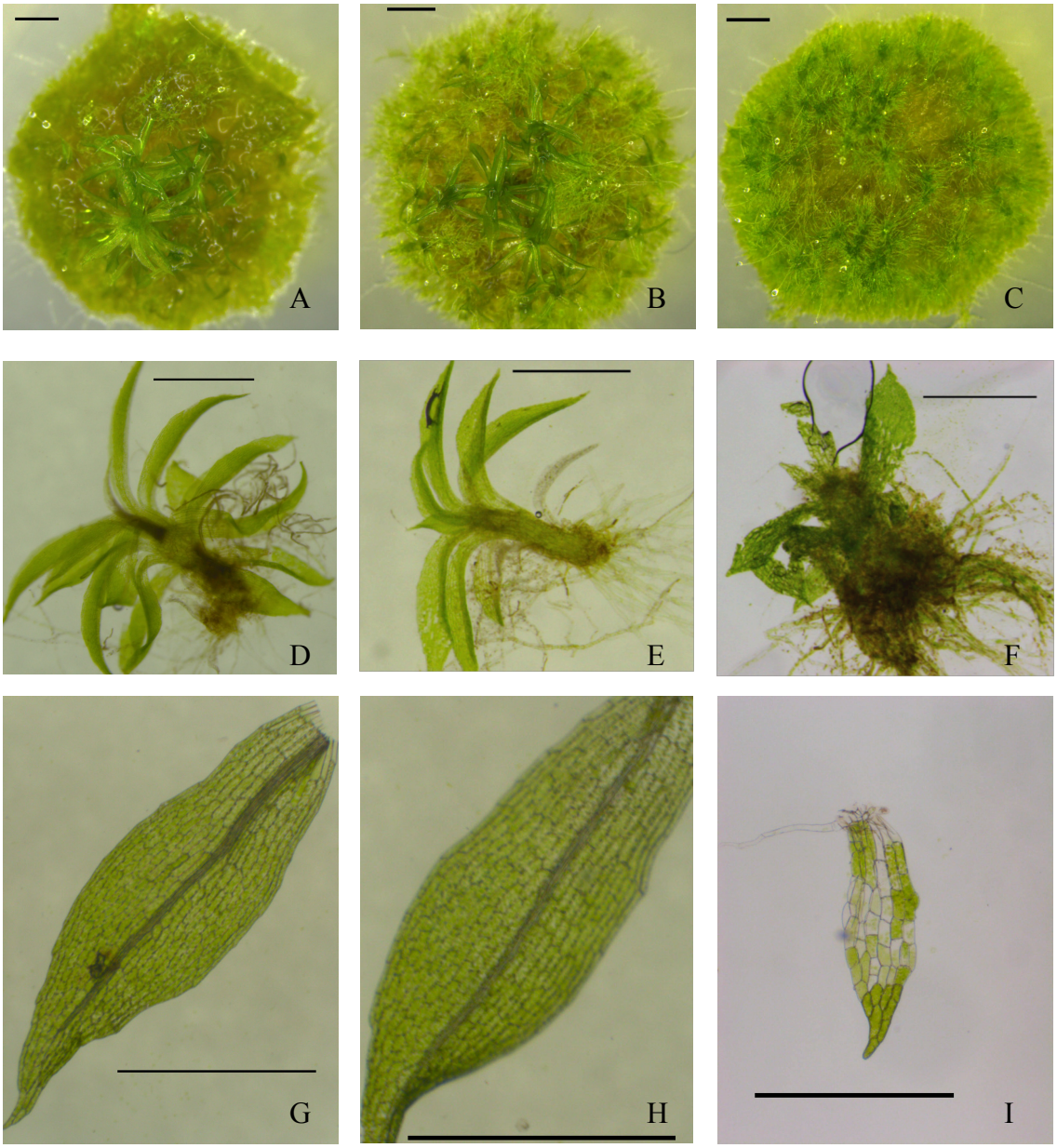

Figure 8. Stably transformed lines from (A) 3XHA*ppcesa5/5/4*, (B) 3XHA*PpCESA5* and (C) xt18-GW. Gametophores from (D) 3XHA*ppcesa5/5/4*, (E) 3XHA*PpCESA5* and (F) xt18-GW. Leaves from (G) 3XHA*ppcesa5/5/4*, (H) 3XHA*PpCESA5* and (I) xt18-GW. 3XHA*ppcesa5/5/4* and 3XHA*PpCESA5* lines resembled the wild type, producing several gametophores per moss line with normal height, phyllotaxy and cell shape and pattern. Xt18-GW lines resembled the *ppcesa5*KO-2B line, producing gametophores rarely with stunted growth, abnormal phyllotaxy and irregular cell shape and pattern. Scale bars are as follows: (A-C) 2mm (D-F) 1 mm (G-I) 0.5mm.

The 3XHA*ppcesa5/5/4*, 3XHA*PpCESA5* and xt18-GW transformed *ppcesa5*KO-2B lines were examined with bright field light microscopy to assess differences in gametophore development. Whole gametophores from 3XHA*ppcesa5/5/4* lines showed no difference in size or phyllotaxy from gametophores from 3XHA*PpCESA5* lines (Figure 8). Closer examination of individual leaves revealed no difference in leaf morphology, nor any difference in cell size, shape and pattern within the leaves (Figure 8).

Expression levels of both transgenes were analyzed through Western blots using an anti-HA antibody and an anti-tubulin antibody. All microsomal protein extracts from twelve lines of 3XHA*ppcesa4/5/5* produced the expected band at 125 kD, indicating that the full-length protein was expressed (Figure 6). In the first blot (Figure 6), all protein extracts from gametophore producing 3XHA*ppcesa5/5/4* lines produced the expected band at 125 kD. Several protein extracts from lines that did not produce gametophores also produced a fainter band at 125 kD. However, it is difficult to determine whether or not protein expression levels are different between gametophore-producing and gametophore-less lines, as anti-tubulin staining shows that protein loading was not properly normalized. In the second blot, all microsomal protein extracts from gametophore producing lines of 3XHA*ppcesa5/5/4* transformed moss, with the exception of the last lane, in which the sample had not been loaded into the well, produced the expected band at 125 kD. Protein from lines that did not produce gametophores did not produce the expected band (Figure 6). However, the presence of the tubulin band (55 kD) is varied in intensity across the samples, indicating that protein levels were not properly normalized. This is most obvious in the positive control, in which neither the HA nor

tubulin band is visible (Figure 6). This opens up the possibility that the transgene is being expressed, but is undetected by the blot.

DISCUSSION

The Experimental Assay

A complementation assay should be able test hypotheses about the function of a specific gene and its encoded product in a reliable and reproducible manner. In order to achieve this, a complementation assay must be based on a mutant with a measurable phenotype that is easy to score. In the *ppcesa5*KO mutants, the phenotype is clear: an inability to form leafy gametophores, only rarely forming stunted, abnormal gametophores (Goss et al. 2012). This phenotype is rescued by the constitutive expression of the disrupted *PpCESA5* gene, demonstrating that this phenotype is the result of a *PpCESA5* deficiency. Additionally, this phenotype is rescued by other *PpCESA*s of the same clade, but not by *PpCESA*s of Clade B (Roberts, unpublished), providing an ideal system in which to test clade-specific functional differences between the *CESA*s. Strengthening this system is the use of positive and negative controls, which provide standards of comparison for statistical analysis. Since constitutive expression of *PpCESA5* in the *ppcesa5*KO-2B line fully rescues the mutant phenotype, an expression vector containing this gene is the ideal positive control. Additionally, the use of the empty destination vector serves as a control for changes in the *ppcesa5*KO phenotype resulting from the transformation process or insertion of vector sequence alone, while simultaneously acting as a standard of comparison for null rescues. To test the functionality of a protein region, it must be possible to modify the region without compromising the functional integrity of the protein as a whole. The use of PCR fusion (Atanassov et al. 2009) adds no recombination or restriction sites between gene fragments, thus maintaining structural integrity and decreasing the likelihood of

misfolding. Additionally, the system must provide a means to test for protein expression levels and integrity. The use of a triple hemagglutinin tag enables the determination of protein expression levels and mass by Western blotting. Protein extracted from the chimeric lines probed with an anti-hemagglutinin antibody indicated that the chimeric genes were indeed being transcribed and translated into proteins of the correct mass.

Due to the high rate of homologous recombination in *P. patens*, it was not necessary to genotype stable transformants. Although not all stable lines transformed with the positive control vector were rescued, statistical analysis comparing test vectors to positive and negative controls enabled testing of complementation with high reliability. We expect that complemented lines resulted from integration of the vector into the 108 locus with no deleterious effect on the phenotype. However, failure to complement in some lines could result from integration of the vector at other loci, which could have an effect on gametophore development independent of the *ppcesa5*KO lesion. It has been reported that PEG-mediated transformation generates a small percentage of polyploidy cells, which are slow-growing (Schaefer and Zryd 1997). Colonies that failed to produce gametophores were often small and it is possible that these lines were polyploid and failed to produce gametophores due to developmental delay. Some stable non-complemented lines may have resulted from integration of a truncated vector that included the resistance marker, but lacked either the *actin1* promoter or the *CESA* coding sequence. This could be tested by variability in protein expression levels across the lines.

In summary, the advantages of the *ppcesa5*KO complementation assay include a) a clear phenotype consisting of abnormal buds and the absence of leafy gametophores, b) the ability to score complementation as either full (normal gametophores), partial

(abundant abnormal gametophores/fewer normal gametophores), or none (no gametophores or very few abnormal gametophores) rescue, c) functional discrimination between the Clade A and Clade B CESAs, d) positive and negative controls for validation of results and comparison of rescues, e) creation of chimeras through PCR fusion without compromising the structural integrity of these closely related proteins, f) the ability to test the expression and integrity of the transgenic proteins through Western blotting with anti-HA and g) the ability to exclude genotyping the mutants.

The CSR is Necessary for Clade-Specific CESA Function

Transformation with an expression vector containing a Clade A *CESA* with the CSR of another Clade A *CESA* (3XHA*ppcesa5CSR8)* rescued the *ppcesa5*KO phenotype (Figure 5 A, Table 3), indicating that CSRs can perform clade-specific functions when inserted into a different CESA from the same clade. Additionally, as the chimeric CESA was not misfolded, this may indicate that the other CSR swaps are unlikely to misfold as well.

The mutant *ppcesa5*KO transformed by an expression vector containing a Clade A *CESA* with the CSR of a Clade B *CESA* (3XHA*ppcesa5CSR4*) did not produce gametophores, retaining the knock out phenotype (Figure 5 B, Table 3). This result supports the hypothesis that the CSR is necessary for clade-specific function, as the change from Clade A CSR to Clade B CSR leads to loss of function of PpCESA5. This may be due to the inability of the chimeric CESA to join a cellulose synthase complex, as supported by the *in silico* modeling of *Gossypium hirsutum* CESA1 catalytic domains as oligomers (Sethaphong et al. 2013). However, it may also be due to the inability of the chimeric CESA to interact with other non-CESA proteins, as the proteins necessary for

CSC formation and function are still unknown (Delmer 1999; Doblin et al. 2002; Guerriero et al. 2010). Alternatively, the CSR may play a previously unidentified role in CESA function unrelated to protein-protein interactions. Although misfolding of the transgenic protein cannot be ruled out, Western blotting results indicate that the transgene is transcribed and translated to produce a protein of the expected mass that is not rapidly degraded. In order to determine whether or not the CSR is involved in CSC formation, it would be useful to perform co-immunoprecipitation experiments on wild type *P. patens* and 3XHA*ppcesa5CSR4* lines. To further test the hypothesis that the CSR is responsible for clade specific function, it would be useful to transform *ppcesa5*KO-2B lines with *PpCESA5* with the CSR of the third Clade A gene (*PpCESA3*) in addition to *PpCESA5* with the CSRs of the untested Clade B genes (*PpCESA7* and *PpCESA10*). This would demonstrate whether the clade-specific function of the CSR is consistent across all *P. patens* CESAs, and not simply CESAs 4, 5 and 8.

The CSR is Not Sufficient for Clade-Specific CESA Function

Transformation with an expression vector containing a Clade B *CESA* with the CSR of a Clade A *CESA* (3XHA*ppcesa4CSR5*) did not rescue the *ppcesa5*KO phenotype, predominantly producing no gametophores and only occasionally producing malformed gametophores consistent with the knock out phenotype (Figure 5 C, Table 3). Transformed lines all produced the expected band at 125 kD (Figure 6) in Western blots. The inability of the *PpCESA5* CSR to confer Clade A-specific function on a Clade B CESA suggests that whereas the CSR is important for clade-specific CESA function in *P. patens*, it is not sufficient. It follows that other CESA features are also required for clade-specific function. To further test this hypothesis, it would be useful to transform

*ppcesa5*KO-2B lines with *PpCESA4* with the CSRs of *PpCESA 8* and *PpCESA3*. Until these tests are performed, it remains possible that one of the Clade CSRs is sufficient to confer Clade A-specific function. If the CSR is not sufficient, then this complementation system could be used to determine the region or regions that are also necessary for clade-specific functions.

The N-terminus is Required for Clade-Specific CESA Function

Transformation with an expression vector containing the N-terminus of a Clade B *CESA* and the CSR and C-terminus of a Clade A *CESA* (3XHA*ppcesa4/5/5*) did not rescue the *ppcesa5*KO phenotype (Table 3, Figure 7 A). Transformed lines all produced the predicted band (Figure 6) in Western blots, indicating that the transgene was transcribed and translated into a full-length protein. These results indicate that at least one feature of the N-terminal segment, including the zinc-binding domain and the P-CR, is necessary for clade-specific function. This is supported by an earlier study in *Arabidopsis thaliana* where CESAs from two different classes, *AtCESA1* and *AtCESA3* were fused such that the N-terminal region of *AtCESA1* (up to the catalytic domain) was fused with the C-terminal region of *AtCESA3* (including the catalytic domain) and used to transform both *atcesa1* and *atcesa3* knock outs. The chimera was only able to rescue *atcesa3* knockouts, indicating that class-specific CESA function in Arabidopsis is attributed to regions in the C-terminus encompassing the catalytic domain (Wang et al. 2006). Coupled with the results of this thesis, this indicates that regions in the catalytic domain are potentially involved in clade-specific function. Based on the results of Wang's experiments, one hypothesis is that the P-CR and CSR must be compatible. Fusing the P-

CR and CSR of a Clade A CESA to the remainder of a Clade B CESA and using the expression vector in the *ppcesa5* KO complementation assay could test this hypothesis.

*Incomplete Rescue by 3XHA*ppcesa5/5/4

Normal gametophores were produced by mutant *ppcesa5*KO lines transformed with an expression vector containing the N-terminus and CSR of a Clade A *CESA* and the C-terminus of a Clade B *CESA* (3XHA*ppcesa5/5/4*, Figure 7 B, Table 3), indicating that the C-terminal portion of all PpCESAs may be able to support clade-specific function. However, fewer colonies from these transformations produced gametophores, suggesting that the chimera may not be fully functional. Every line of the 3XHA*ppcesa5/5/*4 transformants that produced gametophores also produced the expected 125 kD band, with the exception of one in which the protein sample was not loaded into the well. However, three lines that did not produce gametophores produced a weaker 125 kD band (Figure 6). The incomplete rescue of this chimera could be attributed to a fully functional protein that was expressed at a lower level in *ppcesa5*KO than the 3XHA*PpCESA5* and 3XHA*ppcesa5CSR8* chimeras. This is supported by the lower level of transgene expression relative to tubulin expression (Figure 6), although it is difficult to tell due to uneven protein loading. The presence of gametophores could be due to a dosage effect, in which a certain amount of the transgene is required to rescue the *ppcesa5*KO phenotype, as mentioned above. Alternatively, the protein may lack functional integrity, such as a higher propensity for misfolding. In order to test for a dosage effect and functional integrity, Western blots with higher protein concentrations that are properly normalized could reveal a lesser intensity in lines that do not produce gametophores, indicating a

dosage effect or truncated proteins, which would indicate a higher rate of protein misfolding and thus suggest a lack of functional integrity.

Future Directions

This thesis demonstrates that while the CSR is necessary for clade-specific function, it is not sufficient, indicating that one or more other features of the Clade A CESAs are necessary for clade-specific function. Further tests have narrowed down other necessary region or regions as residing in the N-terminal portion of the CESA up to the CSR. Given that the zinc-binding domain, the Plant Conserved Region and the Class Specific Regions are unique to rosette-forming CESAs (Delmer 1999; Doblin et al. 2002; Sethaphong et al. 2013) and that the zinc-binding domain and P-CR occur in the N-terminal region up to the CSR, it seems likely that one or both of these regions are necessary for clade-specific function and possibly CSC formation. In particular, compatibility between the P-CR and CSR, as suggested by *G. hirsutum in silico* models (Sethaphong et al. 2013), may be necessary for clade-specific function. This could be tested by creating swaps of the P-CR and zinc-binding domain between CESAs of Clade A and B to test in the *ppcesa5*KO complementation system. Upon the results of these proposed swaps, it would be useful to create swaps of the other necessary region(s) along with the CSR between CESAs of Clade A and B to test in the *ppcesa5*KO complementation system. Additionally, it would be useful to determine if the clade-specific function that the CSR and other regions have is in CSC formation through co-immunoprecipitation assays.

APPENDIX 1: List of Abbreviations

GT: Glycosyltransferase

CESA: Streptophyte cellulose synthase

CSC: Cellulose synthase complex

CSR: Clade-Specific Region

P-CR: Plant Conserved Region

WAXS: Wide angle X-ray scattering

SAXS: Small angle X-ray scattering

SANS: Small angle neutron scattering

NMR: Neutron magnetic resonance

PEG: Polyethylene glycol

CESA5CSR4: CESA5 with the CSR of CESA4

CESA5CSR8: CESA5 with the CSR of CESA8

CESA4CSR5: CESA4 with the CSR of CESA5

5/5/4: CESA5 with the C-terminus of CESA4

4/5/5: CESA5 with the N-terminus of CESA5

APPENDIX 2: Alignment of *P. patens* CESAs

```
PpCESA10    MESSPGLLAGSHNRNELVVIRQEG-DGPKPLSYVDSRICQICGDDVGLNMRREIFVACDE
PpCESA4     MKANAGLLAGSHNRNELVIIRQEG-DGPKPLSYVNSHICQICGDDVGLTVEGEMFVACNE
PpCESA6     MEANAGLVAGSHNRNELVVIRQES-DGPRPLSNVNSHICQICGDDVGVTLEGEMFVACTE
PpCESA7     MEANAGLLAGSHNRNELVVIRQEG-DEPRPLSNVNSHICQICGDDVGVTLEGEMFVACTE
PpCESA5     MEANAGLIAGSHNRNELVVLRP-DHEGPKPLSQVNSQFCQICGDDVGVTVDGELFVACFE
PpCESA3     MEANAGLVAGSHNRNELVVIPAEGIHGPRPENQMNELVCQICGDAVGLNQDNELFVACNE
PpCESA8     MEANAGLVAGSHNRNELVVIPAEGIHGPRPENQVNELVCQICGDAVGVNQDNELFVACNE
            *::. **:**********::     . *:* . ::. .****** **:.   *:**** *
PpCESA10    CGFPVCRPCYEYERKDGTQACPQCRTRYKRHKGSPRVKGDDEE-EDSDDLDNEFNHDGDL
PpCESA4     CGFPVCRPCYEYERKDGTQACPQCRTRYRRHKGSPRVKGDDEE-EDTDDLDNEFNHAVNL
PpCESA6     CGFPVCRPCYEYERKDGTQACPQCRTRYRRHKGSPRVKGDDEE-EDTDDLDNEFNHNVDI
PpCESA7     CGFPVCRPCYEYERKDGTQACPQCRTRYRRHKGSPRVKGDDEE-EDTDDLDNEFNHNVDI
PpCESA5     CGFPVCRPCFEYERKEGNQSCPQCKSRYNRQKGSPRVPGDEE-EDDTDDLENEFAL--EM
PpCESA3     CAFPVCRTCYEYERKEGNGVCPHCKTRYKRLKGSLRVPGDDDEEDDLDDLENEFQM----
PpCESA8     CAFPVCRTCYEYERKEGNGVCPHCKTRYKRLKGSARVPGDD-EEDDLDDLENEFEM----
            *.***** *:*****:*.  **:*::**.* *** ** **:   :* ***:***
PpCESA10    GKRDEQQVVDEMLHSQMAYGRDMDVTLS-----AMQPTYPLLTDRHRHTVSVTSDSDAMS
PpCESA4     DNHDKQQVVDEMLHSQMAYGRDTEVMLS-----ATQPRYPLLTDGHRHMVSVTSESNATS
PpCESA6     DKHDKQQVVDEMLHSQMAYGRDTDVMMS-----AMQPQYPLLTDGHT--VSGAGESNATS
PpCESA7     DKHDKQQVVDEMLHSQMAYGRDTDVMMS-----AMQPQYPLLTDGHT--VSGAGESNATS
PpCESA5     GQLDEQNVTDAMLHGHMSYGGNYDHNLP---NLHQTPQFPLLTDGKMGDLDDD------S
PpCESA3     DKQDQQPSPDAMLHGRMSYGSMYEQEMATHRMMHQQPRFPLITDGQVGDSEED------E
PpCESA8     DKKDQQPSPDAMLHGRMNYGRMYEHEMATHHMMHQQPRFPLITDGQVGDSEDD------E
             : *:*   * ***.:* **   :  :         * :**:** :    .        .
PpCESA10    PDRQAIFPVTGRRLTHATSYSDIGTP--VRALDSAKDAGSDGYGNVVWKERVESWKSRQG
PpCESA4     PDHQAIFHVAGGKGSHTVSYSDIGSP--ARSLDPAKDLGSYGYGSIAWKERVESWKLRQG
PpCESA6     PDHQAIFPVAGGKRIHPVAYSDIGSP--ARPLDPAKDLGSYGYGSIAWKERVESWKLRQG
PpCESA7     PDHQAIFPVAGGKRIHPVAYSDIGSP--ARPLDPAKDLGSYGYGSIAWKERVESWKLRQG
PpCESA5     HAIVLPPPMNGGKRVHPLPYIESNLPVQARPMDPTKDLAAYGYGSVAWKDRVESWKMRQE
PpCESA3     NHA-LVVPSNGNKRVHPINYMDPNLPVQARPMDPTKDLAAYGYGSVAWKDKVENWKQRQE
PpCESA8     NHA-LVVPSNSNKRVQPINYMDSNLPVQARPMDPSKDLAAYGYGSVAWKDKVDSWKQRQE
               . :  :   * :   *  .* :* :** .: ***.:.**::*:.** **
PpCESA10    MQMTMR-EGGQLQASGEGGYDGSGLDCSDLPIMDESRQPLSRKVPFPSSKINPYRMIIVI
PpCESA4     MQMTTT-AGGQLQANGKGGDDGSHQDCSDLPIMDESRQPLSRKVPFPSSKINPYRMIIVI
PpCESA6     MQMTTT-EGGQLQASGKGGHDENGPDCPDLPIMDESRQPLSRKVPIPSSKINPYRMIIVI
PpCESA7     MQMTTT-EGGQLQASGKGGHDENGPDCPDLPIMDESRQPLSRKVPIPSSKINPYRMIIVI
PpCESA5     KMMT---EGSHHHK----GGDMDGDNGPDLPIMDEARQPLSRKVPISSARINPYRMLIVI
PpCESA3     KMQMMMSEGGVLHP-----SDM-DLNDPDLPIMDESRQPLSRKIPLASSKINPYRMVIVI
PpCESA8     KMQMMMSEGGVLHP-----SDV-DPNGPDLPIMDESRQPLSRKIPIASSRINPYRMVIVI
                  *.  :       *    :  *******:*******:*: *::******:***
PpCESA10    RLVVICLFFRYRILNPVNEAYGLWLVSVICEIWFGISWILDQFPKWLPINRETYLDRLSL
PpCESA4     RLVVICLFFRYRILNPVNEAYGLWLVSVICEIWFGISWILDQFPKWLPINRETYLDRLSL
PpCESA6     RLVVICLFFRYRILNPVNEAYALWLVSVICEIWFAISWILDQFPKWLPINRETYLDRLSL
PpCESA7     RLVVICLFFRYRILNPVNEAYALWLVSVICEIWFAISWILDQFPKWLPINRETYLDRLSL
PpCESA5     RLVVLAFFFRYRILNPVEGAYGMWLTSVICEIWFAISWILDQFPKWLPINRETYLDRLSL
PpCESA3     RLVVLAFFLRYRILHPVEGAFGLWITSVVCEIWFAVSWILDQFPKWLPIQRETYLDRLSL
PpCESA8     RLVVLAFFLRYRILHPVEGAFGLWITSVVCEIWFAVSWILDQFPKWLPIQRETYLDRLSL
            ****:.:*:*****.**: *:.:*:.**:*****.:************:**********
PpCESA10    RFEKEGEPSQLAPVDIYVSTVDPMKEPPLVTANTVLSILAVDYPVDKVSCYISDDGASML
PpCESA4     RFEKEGEPSQLAPVDIYVSTVDPMKEPPLVTANTVLSILAVDYPVDKVSCYISDDGASML
PpCESA6     RFEKEGEPSRLCPVDIYVSTVDPMKEPPLVTANTILSILAVDYPVDKVSCYISDDGASML
PpCESA7     RFEKEGEPSRLCPVDIYVSTVDPMKEPPLVTANTILSILAVDYPVDKVSCYISDDGASML
PpCESA5     RYEKEGEPSQLEHVDIFVSTVDPMKEPPLVTANTILSILAVDYPVDKVSCYLSDDGAAML
PpCESA3     RYEKPGEPSQLAHVDVYVSTVDPLKEPPIVTANTILSILAVDYPVDKVSCYLSDDGAAML
PpCESA8     RYEKPGEPSQLVNVDVYVSTVDPLKEPPIVTANTILSILAVDYPVDKVSCYLSDDGAAML
            *:** ****:*  **::******:****:*****:****************:*****:**
```

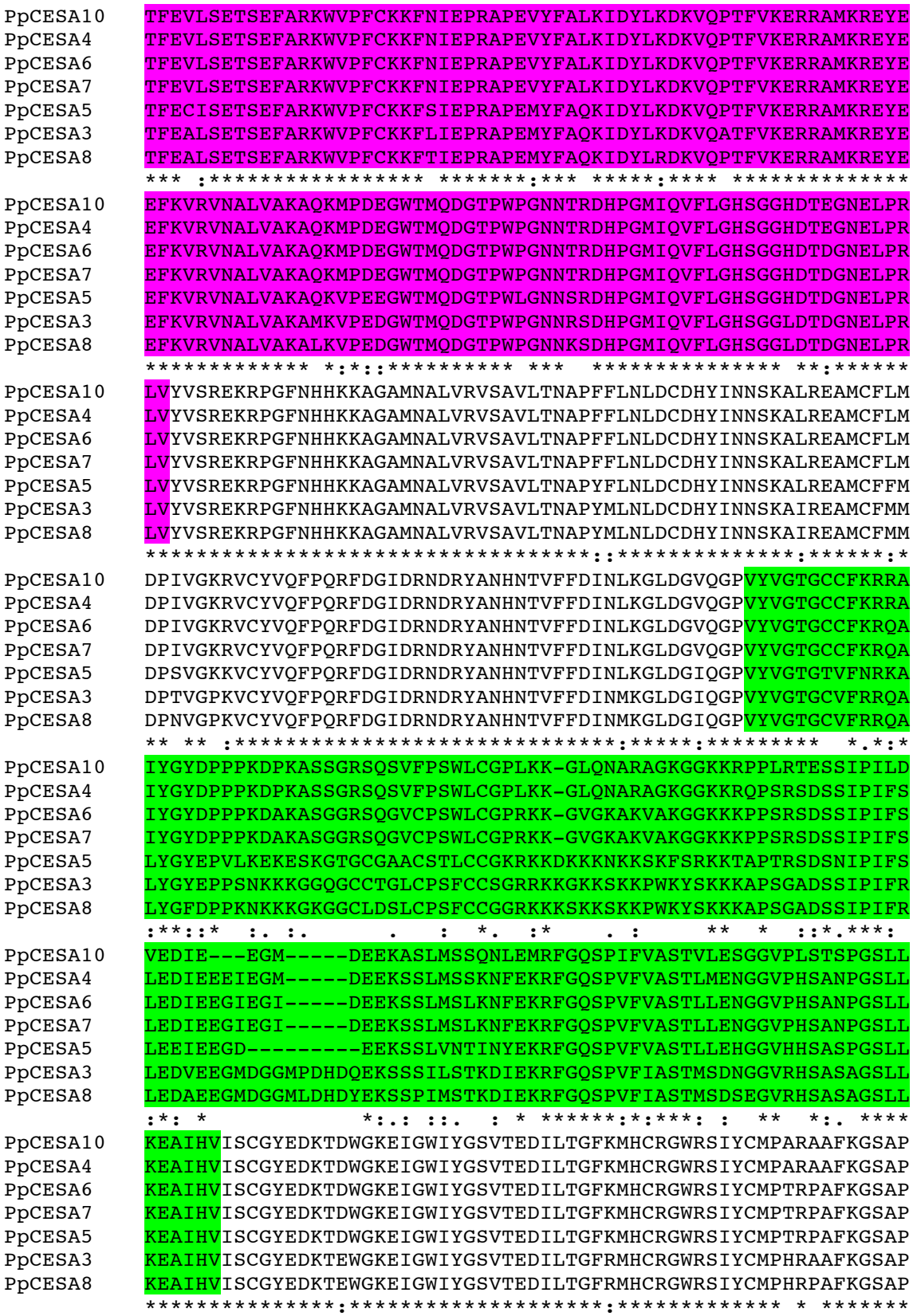
PpCESA10 TFEVLSETSEFARKWVPFCKKFNIEPRAPEVYFALKIDYLKDKVQPTFVKERRAMKREYE
PpCESA4 TFEVLSETSEFARKWVPFCKKFNIEPRAPEVYFALKIDYLKDKVQPTFVKERRAMKREYE
PpCESA6 TFEVLSETSEFARKWVPFCKKFNIEPRAPEVYFALKIDYLKDKVQPTFVKERRAMKREYE
PpCESA7 TFEVLSETSEFARKWVPFCKKFNIEPRAPEVYFALKIDYLKDKVQPTFVKERRAMKREYE
PpCESA5 TFECISETSEFARKWVPFCKKFSIEPRAPEMYFAQKIDYLKDKVQPTFVKERRAMKREYE
PpCESA3 TFEALSETSEFARKWVPFCKKFLIEPRAPEMYFAQKIDYLKDKVQATFVKERRAMKREYE
PpCESA8 TFEALSETSEFARKWVPFCKKFTIEPRAPEMYFAQKIDYLRDKVQPTFVKERRAMKREYE
PpCESA10 EFKVRVNALVAKAQKMPDEGWTMQDGTPWPGNNTRDHPGMIQVFLGHSGGHDTEGNELPR
PpCESA4 EFKVRVNALVAKAQKMPDEGWTMQDGTPWPGNNTRDHPGMIQVFLGHSGGHDTEGNELPR
PpCESA6 EFKVRVNALVAKAQKMPDEGWTMQDGTPWPGNNTRDHPGMIQVFLGHSGGHDTDGNELPR
PpCESA7 EFKVRVNALVAKAQKMPDEGWTMQDGTPWPGNNTRDHPGMIQVFLGHSGGHDTDGNELPR
PpCESA5 EFKVRVNALVAKAQKVPEEGWTMQDGTPWLGNNSRDHPGMIQVFLGHSGGHDTDGNELPR
PpCESA3 EFKVRVNALVAKAMKVPEDGWTMQDGTPWPGNNRSDHPGMIQVFLGHSGGLDTDGNELPR
PpCESA8 EFKVRVNALVAKALKVPEDGWTMQDGTPWPGNNKSDHPGMIQVFLGHSGGLDTDGNELPR
PpCESA10 LVYVSREKRPGFNHHKKAGAMNALVRVSAVLTNAPFFLNLDCDHYINNSKALREAMCFLM
PpCESA4 LVYVSREKRPGFNHHKKAGAMNALVRVSAVLTNAPFFLNLDCDHYINNSKALREAMCFLM
PpCESA6 LVYVSREKRPGFNHHKKAGAMNALVRVSAVLTNAPFFLNLDCDHYINNSKALREAMCFLM
PpCESA7 LVYVSREKRPGFNHHKKAGAMNALVRVSAVLTNAPFFLNLDCDHYINNSKALREAMCFLM
PpCESA5 LVYVSREKRPGFNHHKKAGAMNALVRVSAVLTNAPYFLNLDCDHYINNSKALREAMCFFM
PpCESA3 LVYVSREKRPGFNHHKKAGAMNALVRVSAVLTNAPYMLNLDCDHYINNSKAIREAMCFMM
PpCESA8 LVYVSREKRPGFNHHKKAGAMNALVRVSAVLTNAPYMLNLDCDHYINNSKAIREAMCFMM
PpCESA10 DPIVGKRVCYVQFPQRFDGIDRNDRYANHNTVFFDINLKGLDGVQGPVYVGTGCCFKRRA
PpCESA4 DPIVGKRVCYVQFPQRFDGIDRNDRYANHNTVFFDINLKGLDGVQGPVYVGTGCCFKRRA
PpCESA6 DPIVGKRVCYVQFPQRFDGIDRNDRYANHNTVFFDINLKGLDGVQGPVYVGTGCCFKRQA
PpCESA7 DPIVGKRVCYVQFPQRFDGIDRNDRYANHNTVFFDINLKGLDGVQGPVYVGTGCCFKRQA
PpCESA5 DPSVGKKVCYVQFPQRFDGIDRNDRYANHNTVFFDINLKGLDGIQGPVYVGTGTVFNRKA
PpCESA3 DPTVGPKVCYVQFPQRFDGIDRNDRYANHNTVFFDINMKGLDGIQGPVYVGTGCVFRRQA
PpCESA8 DPNVGPKVCYVQFPQRFDGIDRNDRYANHNTVFFDINMKGLDGIQGPVYVGTGCVFRRQA
PpCESA10 IYGYDPPPKDPKASSGRSQSVFPSWLCGPLKK-GLQNARAGKGGKKRPPLRTESSIPILD
PpCESA4 IYGYDPPPKDPKASSGRSQSVFPSWLCGPLKK-GLQNARAGKGGKKRQPSRSDSSIPIFS
PpCESA6 IYGYDPPPKDAKASGGRSQGVCPSWLCGPRKK-GVGKAKVAKGGKKKPPSRSDSSIPIFS
PpCESA7 IYGYDPPPKDAKASGGRSQGVCPSWLCGPRKK-GVGKAKVAKGGKKKPPSRSDSSIPIFS
PpCESA5 LYGYEPVLKEKESKGTGCGAACSTLCCGKRKKDKKKNKKSKFSRKKTAPTRSDSNIPIFS
PpCESA3 LYGYEPPSNKKKGGQGCCTGLCPSFCCSGRRKKGKKSKKPWKYSKKKAPSGADSSIPIFR
PpCESA8 LYGFDPPKNKKKGKGGCLDSLCPSFCCGGRKKKSKKSKKPWKYSKKKAPSGADSSIPIFR
PpCESA10 VEDIE---EGM-----DEEKASLMSSQNLEMRFGQSPIFVASTVLESGGVPLSTSPGSLL
PpCESA4 LEDIEEEIEGM-----DEEKSSLMSSKNFEKRFGQSPVFVASTLMENGGVPHSANPGSLL
PpCESA6 LEDIEEGIEGI-----DEEKSSLMSLKNFEKRFGQSPVFVASTLLENGGVPHSANPGSLL
PpCESA7 LEDIEEGIEGI-----DEEKSSLMSLKNFEKRFGQSPVFVASTLLENGGVPHSANPGSLL
PpCESA5 LEEIEEGD---------EEKSSLVNTINYEKRFGQSPVFVASTLLEHGGVHHSASPGSLL
PpCESA3 LEDVEEGMDGGMPDHDQEKSSSILSTKDIEKRFGQSPVFIASTMSDNGGVRHSASAGSLL
PpCESA8 LEDAEEGMDGGMLDHDYEKSSPIMSTKDIEKRFGQSPVFIASTMSDSEGVRHSASAGSLL
PpCESA10 KEAIHVISCGYEDKTDWGKEIGWIYGSVTEDILTGFKMHCRGWRSIYCMPARAAFKGSAP
PpCESA4 KEAIHVISCGYEDKTDWGKEIGWIYGSVTEDILTGFKMHCRGWRSIYCMPARAAFKGSAP
PpCESA6 KEAIHVISCGYEDKTDWGKEIGWIYGSVTEDILTGFKMHCRGWRSIYCMPTRPAFKGSAP
PpCESA7 KEAIHVISCGYEDKTDWGKEIGWIYGSVTEDILTGFKMHCRGWRSIYCMPTRPAFKGSAP
PpCESA5 KEAIHVISCGYEDKTDWGKEIGWIYGSVTEDILTGFKMHCRGWRSIYCMPTRPAFKGSAP
PpCESA3 KEAIHVISCGYEDKTEWGKEIGWIYGSVTEDILTGFRMHCRGWRSIYCMPHRAAFKGSAP
PpCESA8 KEAIHVISCGYEDKTEWGKEIGWIYGSVTEDILTGFRMHCRGWRSIYCMPHRPAFKGSAP

```
PpCESA10    INLSDRLQQVLRWALGSVEISLSRHCPLWYGYGGGKHGELKCLERLAYINTTIYPLTSLP
PpCESA4     INLSDRLQQVLRWALGSVEISLSRHCPLWYGYGGGKNGGLKCLERLAYINTTIYPLTSLP
PpCESA6     INLSDRLNQVLRWALGSVEISLSRHCPLWYGYGGGKNGGLKCLERLAYINTTIYPLTSLP
PpCESA7     INLSDRLNQVLRWALGSVEISLSRHCPLWYGYGGGKNGGLKCLERLAYINTTIYPLTSLP
PpCESA5     INLSDRLNQVLRWALGSVEISLSRHCPLWYGYGG----RLKCLERLAYINATIYPLTSLP
PpCESA3     INLSDRLNQVLRWALGSVEISLSRHCPLWFGYG-----RLKCLERLAYINTTIYPLTSLP
PpCESA8     INLSDRLNQVLRWALGSVEISLSRHCPLWYGYG-----RLKCLERLAYINTTIYPLTSLP
            *******:**********************:***      ***********:*********
PpCESA10    LLAYCVLPAVCLLTGKFIIPTITNLDSLWFISLFISIFATGILEMRWSGVGIDEWWRNEQ
PpCESA4     LLAYCVLPAVCLLTGKFIIPTISNLASLWFISLFISIFATGILEMRWSGVGIDEWWRNEQ
PpCESA6     LLAYCVLPAVCLLTGKFIIPTISNLASLWFISLFISIFATGILEMRWSGVGIDEWWRNEQ
PpCESA7     LLAYCVLPAVCLLTGKFIIPTISNLASLWFISLFISIFATGILEMRWSGVGIDEWWRNEQ
PpCESA5     LVAYCVLPAVCLLTGNFIIPTISNLDSLYFISLFLSIFVTGILEMRWSGVGIDEWWRNEQ
PpCESA3     LVAYCTLPAVCLLTGNFIIPTISNLDSLWFISLFMSIFITGILEMRWSGVGIDEWWRNEQ
PpCESA8     LVAYCTLPAVCLLTGKFIIPTISNLDSLWFISLFMSIFITGILEMRWSGVGIDEWWRNEQ
            *:***.*********:******:** **:*****:*** **********************
PpCESA10    FWVIGGVSAHLFALFQGLLKVLAGIDTNFTVTSKQAEDEDFAELYMIKWTALLIPPTTLL
PpCESA4     FWVIGGVSAHLFALFQGLLKVFAGIDTNFTVTSKQAEDEDFAELYMIKWTALLIPPTTLL
PpCESA6     FWVIGGVSAHLFALFQGLLKVFAGIDTNFTVTSKQAEDEDFAELYMIKWTALLIPPTTLI
PpCESA7     FWVIGGVSAHLFALFQGLLKVFAGIDTNFTVTSKQAEDEDFAELYMIKWTALLIPPTTLI
PpCESA5     FWVIGGVSAHLFALFQGLLKVFAGVDTNFTVTSKQADDEDFGELYMLKWTSLLIPPTTIL
PpCESA3     FWVIGGVSAHLFALFQGLLKVFAGIDTNFTVTSKTGEDEDFGELYALKWTSLLIPPTTLL
PpCESA8     FWVIGGVSAHLFALFQGLLKVFAGIDTNFTVTSKTGEDEDFGELYTLKWTSLLIPPTTLL
            **********************:**:********* .:****.*** :***:*******::
PpCESA10    VINMIGVVAGISDAINNGYQSWGPLFGKLFFAFWVIVHLYPFLKGLMGRQNRTPTIVIVW
PpCESA4     VINMIGVVAGISDAINNGYQSWGPLFGKLFFAFWVIVHLYPFLKGLMGRQNRTPTIVIVW
PpCESA6     VINMIGVVAGISDAINNGYQSWGPLFGKLFFAFWVIVHLYPFLKGLMGRQNRTPTIVIVW
PpCESA7     VINMIGVVAGISDAINNGYQSWGPLFGKLFFAFWVIVHLYPFLKGLMGRQNRTPTIVIVW
PpCESA5     ILNLVGVVAGISDAINNGYQSWGPLFGKLFFAFWVIVHLYPFLKGLMGRQNRTPTIVIVW
PpCESA3     IFNMVGVVAGISDAINNGYSAWGPLFGKLFFAFWVIVHLYPFLKGLMGRQNRTPTIVIVW

PpCESA8     LFNMVGVVAGISDAINNGYSAWGPLFGKLFFAFWVIVHLYPFLKGLMGRQNRTPTIVIVW
            ::*::***************.:**************************************
PpCESA10    SILLASIFSLLWVRIDPFLAKVTGPDITECGINC-
PpCESA4     SILLASIFSLLWVRIDPFLAKVKGPDLSQCGINCR
PpCESA6     SILLASIFSLLWVRIDPFLAKVKGPDLSQCGINC-
PpCESA7     SILLASIFSLLWVRIDPFLAKVKGPDLSQCGINC-
PpCESA5     SILLASIFSLLWVRINPFLSRSNGPNLVECGLSC-
PpCESA3     SILLASIFSLLWVRIDPFLPKVTGPNLVRCGLTCL
PpCESA8     SILLASIFSLLWVRIDPFLPKSTGPNLVRCGLTCL
            ***************:*** : .**:: .**:.*
```

Alignment of four Clade B CESAs are (top) and three Clade A CESAs (bottom) via Clustal Omega (European Molecular Biology Labs-European Bioinformatics Institute, Cambridge, UK, http://www.ebi.ac.uk/Tools/msa/clustalo/). The zinc-binding domain is highlighted in blue, the P-CR is highlighted in purple, the CSR is highlighted in green. Stars indicate a conserved residue while colons indicate a similar structure. Periods indicate a relatively similar size and blank spaces indicate no conservation.

APPENDIX 3: CSR Alignment and Helix Prediction

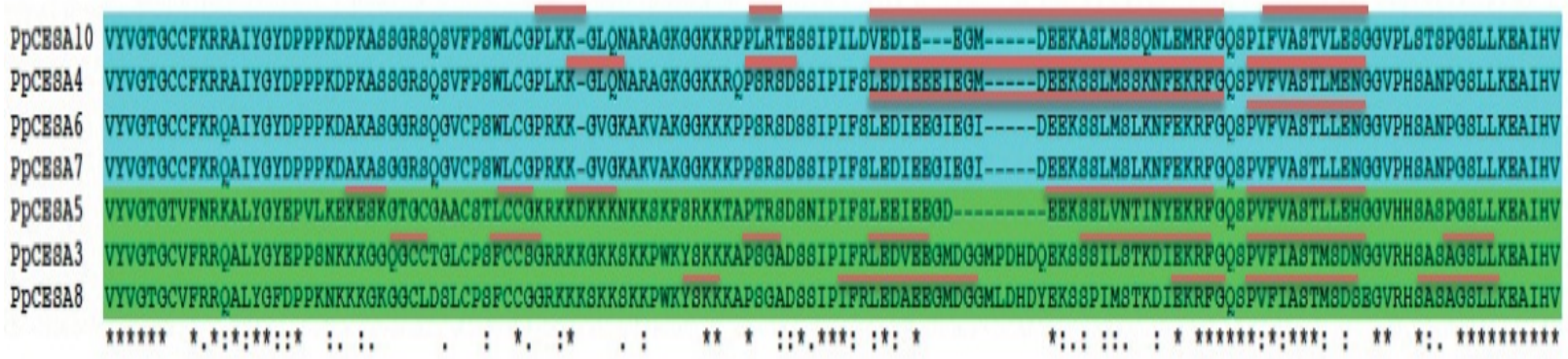

Alignment of four Clade B CESAs are (top) and three Clade A CESAs (bottom) via Clustal Omega (European Molecular Biology Labs-European Bioinformatics Institute, Cambridge, UK, http://www.ebi.ac.uk/Tools/msa/clustalo/).Red lines indicate α-helices as predicted by *in silico* modeling (Sethaphong, unpublished). PpCESA7 helices not shown because the CSR amino acid sequence is identical for that of PpCESA6.

APPENDIX 4: PCR Fusion Protocol

Fusion reaction schematic with fragments and primers labeled:

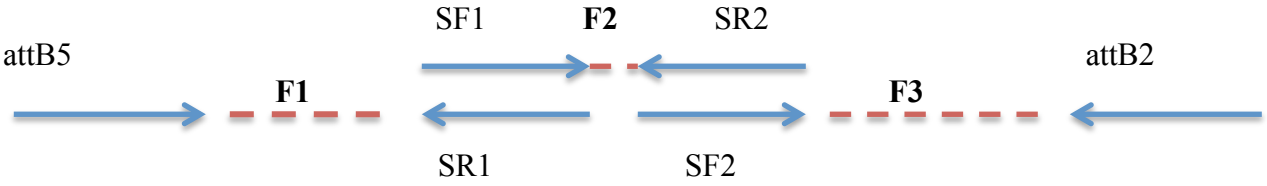

Procedure:

1. Program thermocycler as follows for standard Phusion polymerase (hot start step can be deleted if using Phusion HS).

Hot Start – 98C
Initial Denaturation – 98C, 30s
Denaturation – 98C, 8s
Annealing – 68C, 25s
Extension – 72C, 1 min
} 30 cycles
Final Extension – 72C, 5 min
Hold – 4C

2. Prepare PCR reactions for two or three fragment fusion according to the tables below and amplify:

Ingredient	**Reaction F1**	**Reaction F2**	**Reaction F3**
PCR grade water	34.5 µl	34.5 µl	34.5 µl
HF Phusion Buffer	10 µl	10 µl	10 µl
dNTP mix (10 mM each)	1 µl	1 µl	1 µl
Forward primer (25 µM)	1 µl (CESA attB5)	1 µl (SF1)	1 µl (SF2)
Reverse primer (25 µM)	1 µl (SR1)	1 µl (SR2)	1 µl (CESA attB2)
Template DNA (1 ng/µl)	2 µl	2 µl	2 µl
Phusion polymerase	0.5 µl	0.5 µl	0.5 µl

A gel with estimated concentrations and suggested amounts for PCR fusion reaction:

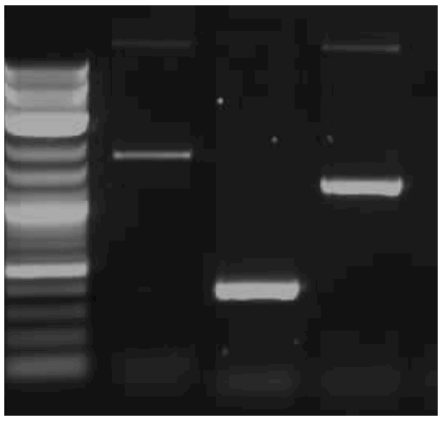

60 ng 120 ng 120 ng
6.67 µl 0.67 µl 1.67 µl

If they are correct, proceed to PCR fusion:

- Make sure that your total DNA mass does not exceed 800 ng.
- Make sure that the mass (ng) of each fragment is proportional to its size. Ex: F1 is 2000 bp, F2 is 400 bp and F3 is 1000 bp, so you will use 400 ng of F1, 80 ng of F2 and 200 ng of F3 (680 ng total < 800 ng).

PCR Fusion Mix:
6 µl HF Phusion Buffer
0.3 µl Phusion enzyme
0.3 µl dNTP (10 ng/µl)
F1, F2, F3 (3 fragment) or F1 & F2 (2 fragment) up to 800 ng
Add ddH2O to bring the remaining volume to 30 µl

Thermocycler conditions:
Hot Start – 98C
Denaturation – 98C, 30s
Annealing – 60C, 1 min
Extension – 72C, 7 min
Hold – 4C

After this step, PEG purify the PCR products:

70 µl 1XTE
30 µl PCR product
50 µl 30% PEG/MgCl2
Vortex & centrifuge at 15,000 rpm for 15 minutes. Slowly pipette off supernatant.
Resuspend in 7 µl 1XTE.

Use 3.5 µl of PCR product per BP reaction (add 0.5 µl pDONR – 75ng).

APPENDIX 5: Individual Trials of N- and C-Terminal Swaps

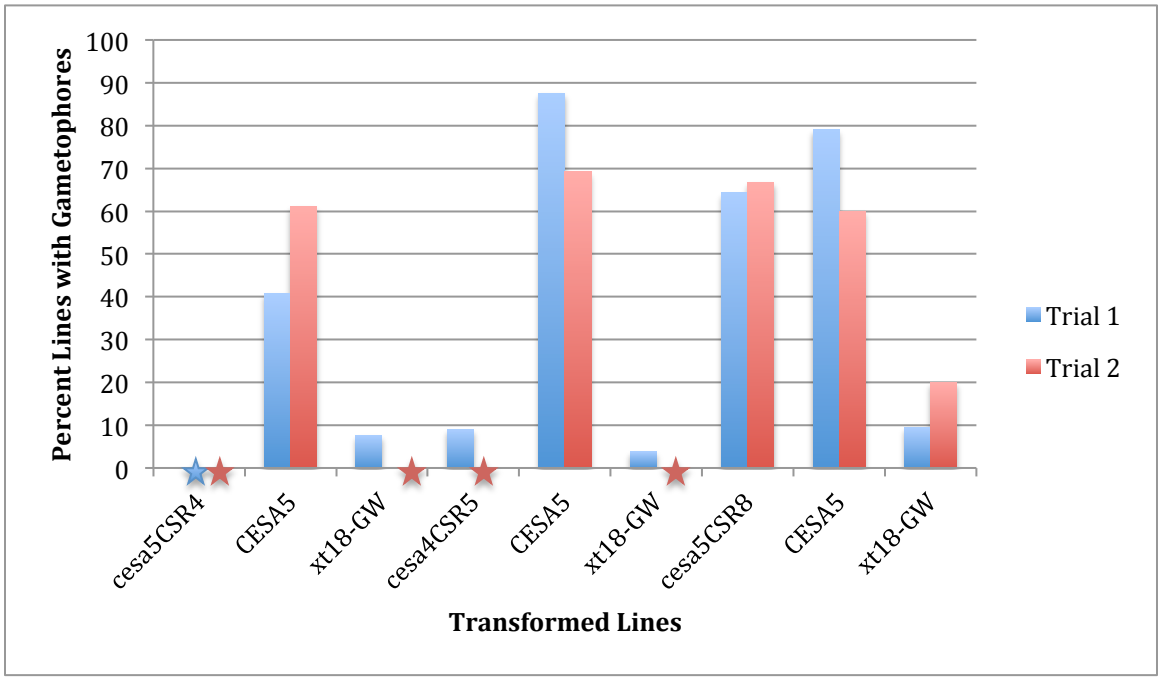

Individual trials of *ppcesa5*KO-2B phenotypic rescue by (from left to right): Clade A CESA with Clade B CSR, Clade B CESA with Clade A CSR, Clade A CESA with Clade A CSR and corresponding positive and negative control vectors. Stars indicate a value of zero.

APPENDIX 6: Western Blots

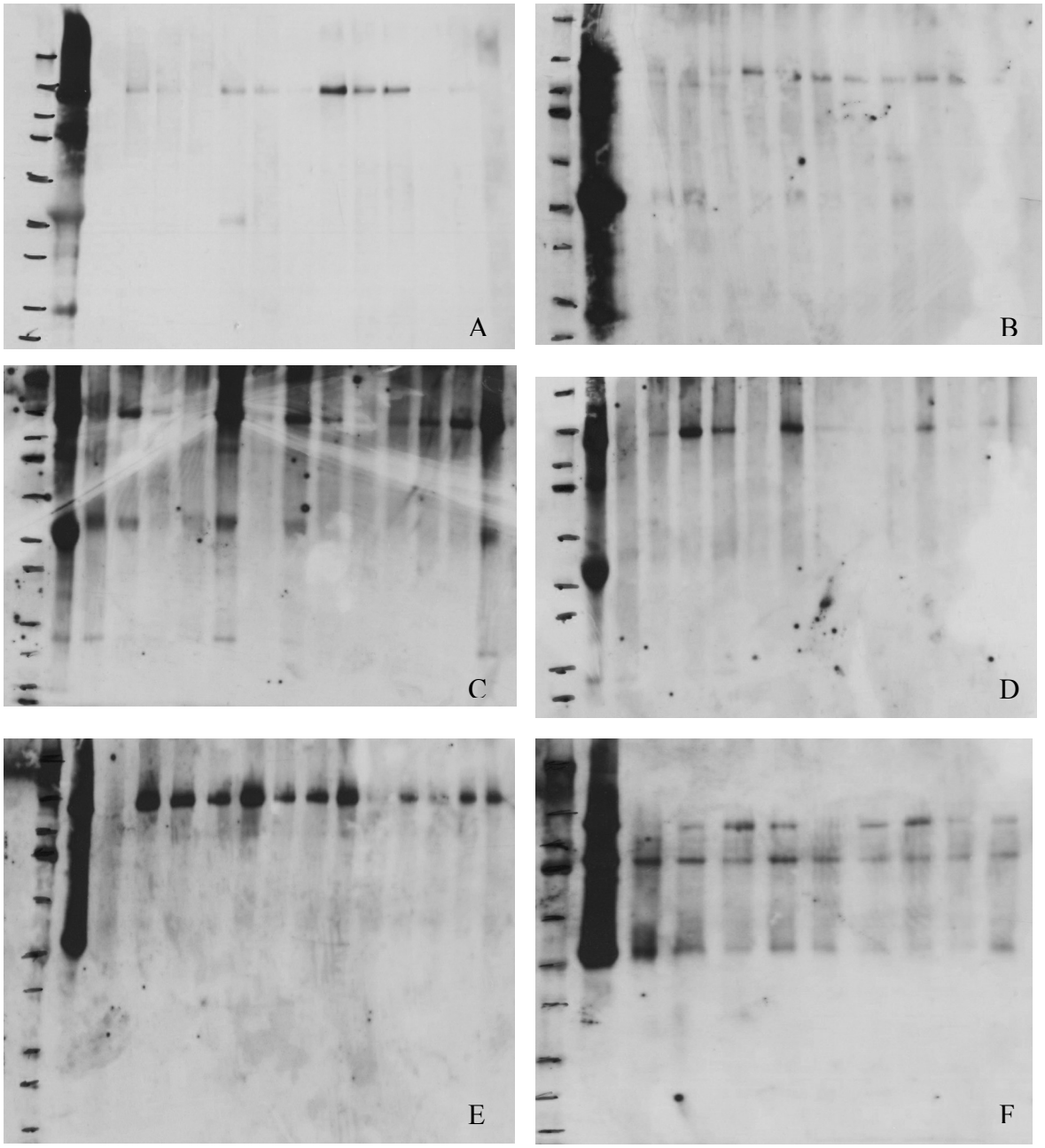

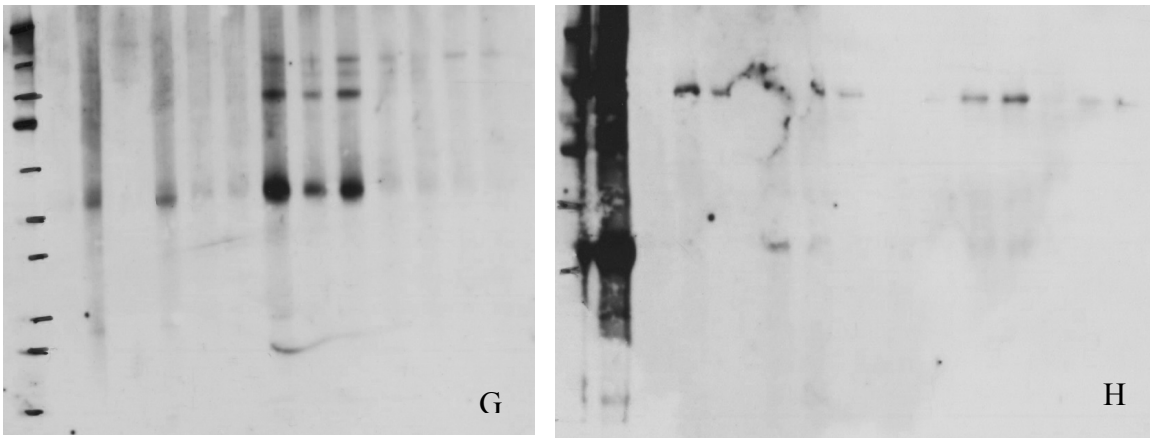

Western blots of microsomal protein extracts from *ppcesa5*KO-2B lines transformed with expression vectors containing various 3XHA-CESA fusions. Blots were probed with an anti-HA antibody and an anti-tubulin antibody. The Novex Sharp Standard (Life Technologies) was used to determine molecular weights. Western blots of vectors containing (A) 3XHA*PpCESA5*, (B) 3XHA*PpCESA5*, (C) 3XHA*ppcesa4CSR5*, (D) 3XHA*ppcesa5CSR4*, (E) 3XHA*ppcesa4/5/5*, (F) 3XHA*ppcesa5/5/4*, (G) 3XHA*ppcesa5/5/4* and (H) 3XHA*ppcesa5/5/4*.

BIBLIOGRAPHY

Arioli T (1998) Molecular analysis of cellulose biosynthesis in Arabidopsis. Science 279: 717-720

Atanassov II, Atanassov II, Etchells JP, Turner SR (2009) A simple, flexible and efficient PCR-fusion/Gateway cloning procedure for gene fusion, site-directed mutagenesis, short sequence insertion and domain deletions and swaps. Plant methods 5: 14

Carroll A, Somerville C (2009) Cellulosic biofuels. Annual review of plant biology 60: 165-182

Cove D (2005) The moss Physcomitrella patens. Annual Review of Genetics 39: 339-358

Delmer D (1999) Cellulose biosynthesis: Exciting times for a difficult field of study. Annual Review of Plant Physiology and Plant Molecular Biology 50: 245-276

Desprez T, Juraniec M, Crowell EF, Jouy H, Pochylova Z, Parcy F, Hofte H, Gonneau M, Vernhettes S (2007) Organization of cellulose synthase complexes involved in primary cell wall synthesis in Arabidopsis thaliana. Proceedings of the National Academy of Science U S A 104: 15572-15577

Doblin MS, Kurek I, Jacob-Wilk D, Delmer DP (2002) Cellulose biosynthesis in plants: from genes to rosettes. Plant Cell Physiology 43: 1407-1420

Goss CA, Brockmann DJ, Bushoven JT, Roberts AW (2012) A CELLULOSE SYNTHASE (CESA) gene essential for gametophore morphogenesis in the moss Physcomitrella patens. Planta 235: 1355-1367

Guerriero G, Fugelstad J, Bulone V (2010) What do we really know about cellulose biosynthesis in higher plants? Journal of integrative plant biology 52: 161-175

Ha M-A, Apperley DC, Evans BW, Jardine WG, Vietor RJ, Reis D, Vian B, Jarvis MC (1998) Fine structure in cellulose microfibrils: NMR evidence from onion and quince. The Plant Journal 16: 183-190

Herth W (1983) Arrays of plasma-membrane "rosettes" involved in cellulose microfibril formation of Spirogyra. Planta 159: 347-356

Hutton JL, Knight CD, Millner PA (1998) The Physcomitrella patens GPa1 homologue is located at
protonemal cell junctions. Journal of Experimental Botany 49: 1113-1118

Ihara Y, Sakai F, Hayashi T (1997) Cloning of homologs of bcsA gene from developing cotton fiber cells. Wood Research 84: 1-6

Kimura S, Laosinchai W, Itoh T, Cui X, Linder CR, Brown J, R. M. (1999) Immunogold labeling of rosette terminal cellulose-synthesizing complexes in the vascular plant Vigna angularis. The Plant Cell 11: 2075-2085

Morgan JL, Strumillo J, Zimmer J (2013) Crystallographic snapshot of cellulose synthesis and membrane translocation. Nature 493: 181-186

Mueller SC, Brown J, R. M. (1980) Evidence for an intramembrane component associated with a cellulose microfibril-synthesizing complex in higher plants. Journal of Cell Biology 84: 315-326

Newman RH, Hill SJ, Harris PJ (2013) Wide-angle x-ray scattering and solid-state nuclear magnetic resonance data combined to test models for cellulose microfibrils in mung bean cell walls. Plant physiology 163: 1558-1567

Pear JR, Kawagoe Y, Schreckengost WE, Delmer DP, Stalker DM (1996) Higher plants contain homologs of the bacterial celA genes encoding the catalytic subunit of cellulose synthase. Proceedings of the National Academy of Sciences U S A 93: 12637-12642

Perroud PF, Quatrano RS (2006) The role of ARPC4 in tip growth and alignment of the polar axis in filaments of Physcomitrella patens. Cell Motility and Cytoskeleton 63: 162-171

Persson S, Paredez A, Carroll A, Palsdottir H, Doblin M, Poindexter P, Khitrov N, Auer M, Somerville CR (2007) Genetic evidence for three unique components in primary cell-wall cellulose synthase complexes in Arabidopsis. Proceedings of the National Academy of Sciences U S A 104: 15566-15571

Rensing SA, Lang D, Zimmer AD, Terry A, Salamov A, Shapiro H, Nishiyama T, Perroud PF, Lindquist EA, Kamisugi Y, Tanahashi T, Sakakibara K, Fujita T, Oishi K, Shin IT, Kuroki Y, Toyoda A, Suzuki Y, Hashimoto S, Yamaguchi K, Sugano S, Kohara Y, Fujiyama A, Anterola A, Aoki S, Ashton N, Barbazuk WB, Barker E, Bennetzen JL, Blankenship R, Cho SH, Dutcher SK, Estelle M, Fawcett JA, Gundlach H, Hanada K, Heyl A, Hicks KA, Hughes J, Lohr M, Mayer K, Melkozernov A, Murata T, Nelson DR, Pils B, Prigge M, Reiss B, Renner T, Rombauts S, Rushton PJ, Sanderfoot A, Schween G, Shiu SH, Stueber K, Theodoulou FL, Tu H, Van de Peer Y, Verrier PJ, Waters E, Wood A, Yang L, Cove D, Cuming AC, Hasebe M, Lucas S, Mishler BD, Reski R, Grigoriev IV, Quatrano RS, Boore JL (2008) The Physcomitrella genome reveals evolutionary insights into the conquest of land by plants. Science 319: 64-69

Roberts AW, Bushoven JT (2007) The cellulose synthase (CESA) gene superfamily of the moss Physcomitrella patens. Plant Molecular Biology 63: 207-219

Roberts AW, Dimos CS, Budziszek MJ, Jr., Goss CA, Lai V (2011) Knocking out the wall: protocols for gene targeting in Physcomitrella patens. Methods in molecular biology 715: 273-290

Rohl CA, Strauss CEM, Misura KMS, Baker D (2004) Protein structure prediction using Rosetta. Methods in Enzymology 383: 66-93

Saxena IM, Brown J, R. M., Fevre M, Geremia RA, Henrissat B (1995) Multidomain architecture of B-glycosyl transferases: Implications for mechanism of action. Journal of Bacteriology 177: 1419-1424

Schaefer DG, Zryd JP (1997) Efficient gene targeting in the moss Physcomitrella patens. . The Plant Journal 11: 1195-1206

Sethaphong L, Haigler CH, Kubicki JD, Zimmer J, Bonetta D, DeBolt S, Yingling YG (2013) Tertiary model of a plant cellulose synthase. Proceedings of the National Academy of Sciences U S A 110: 7512-7517

Sokal RR, Rohlf FJ (1981) Biometry. W. H. Freeman and Company, New York

Sturcova A, His I, Apperley DC, Sugiyama J, Jarvis MC (2004) Structural details of crystalline cellulose from higher plants. Biomacromolecules 5: 1333-1339

Taylor NG, Howells RM, Huttly AK, Vickers K, Turner SR (2003) Interactions among three distinct CesA proteins essential for cellulose synthesis. Proceedings of the National Academy of Science U S A 100: 1450-1455

Thomas LH, Forsyth VT, Sturcova A, Kennedy CJ, May RP, Altaner CM, Apperley DC, Wess TJ, Jarvis MC (2013) Structure of cellulose microfibrils in primary cell walls from collenchyma. Plant physiology 161: 465-476

Vergara CE, Carpita NC (2001) β-D-Glycan synthases and the CesA gene family: lessons to be learned from the mixed-linkage (1→3),(1→4) β -D-glucan synthase. Plant Molecular Biology 47: 145-160

Wada M, Heux L, Sugiyama J (2004) Polymorphism of cellulose I family: Reinvestigation of cellulose IV. Biomacromolecules 5: 1385-1391

Wang J, Howles PA, Cork AH, Birch RJ, Williamson RE (2006) Chimeric proteins suggest that the catalytic and/or C-terminal domains give CesA1 and CesA3 access to their specific sites in the cellulose synthase of primary walls. Plant physiology 142: 685-695

Zhong R, Morrison WH, 3rd, Freshour GD, Hahn MG, Ye ZH (2003) Expression of a mutant form of cellulose synthase AtCesA7 causes dominant negative effect on cellulose biosynthesis. Plant physiology 132: 786-795